Electronic Supplementary Information

From glucose to enantiopure morpholino β-amino acid: a new tool for stabilizing γ-turns in peptides

Raffaella Bucci, Alessandro Contini,* Francesca Clerici, Sara Pellegrino, Maria Luisa Gelmi*

DISFARM-Sez. Chimica Generale e Organica "A. Marchesini", Università degli Studi di Milano, via Venezian 21, 20133 Milano, Italy

1. Experimental materials and methods

Melting points were determined with a Stuart Scientific melting point apparatus in open capillary tubes and are uncorrected. Chemicals were purchased from Sigma Aldrich and were used without further purification. HPLC analysis were performed on Jasco PU-980 pump equipped with a UV–vis detector Jasco UV-975 (wavelength: 220 nm) and on a Kromasil 5-AmyCoat column (4.6 mm i.d. × 250 mm, 5 μm, AkzoNobel). Mass spectra were recorded on an LCQESI MS were recorded on a LCQ Advantage spectrometer from Thermo Finningan and a LCQ Fleet spectrometer from Thermo Scientific. The NMR spectroscopic experiments were carried out either on a Varian MERCURY 200 MHz (200 and 50 MHz for ^{1}H and ^{13}C, respectively), Varian MERCURY 200 MHz (300 and 75 MHz for ^{1}H and ^{13}C, respectively), or Bruker Avance I 500 MHz spectrometers (500 and 125 MHz for ^{1}H and ^{13}C, respectively). Optical rotations were measured on a Perkin–Elmer 343 polarimeter at 20°C (concentration in g/100 mL). Chemical shifts δ are given in ppm relative to the $CHCl_3$ internal standard, and the coupling constants J are reported in Hertz (Hz).

The synthesis of dipeptides NH_2-Leu-Val-$CONH_2$ (**6a**),[1] NH_2-Leu-Val-OBn (**6b**)[1] and *N*-Boc-Val-Gly-OH (**9**)[2] are reported in the literature.

2*S*,6*S*-(4-Benzyl-6-methoxymorpholin-2-yl)methanol (3).

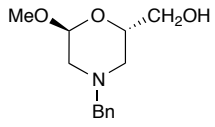

(+)-**3**

3-Hydroxy-2-(1-methoxy-2-oxoethoxy)propanal intermediate **A** was prepared according to the know procedure.[3] Compound **A** was immediately used without further purification for the preparation of compound **3.** In a two-neck round-bottom flask, equipped with magnetic stirrer and nitrogen inlet, compound **2** (1.7 g, 10.6 mmol) was dissolved in MeOH (80 mL). $NaBH_3CN$ (1.12 g, 17.6 mmol) and benzylamine (0.4 mL, 3.6 mmol) were added at 0 °C and the pH was adjusted to 7 with AcOH. The solution was stirred overnight at 25 °C and then benzylamine (0.8 mL, 7 mmol) was added and the pH was newly adjusted to 7. After 16 h, the reaction was concentrated *in vacuo* and the crude was dissolved in AcOEt (30 mL). The organic layer was washed with water (5 x 30 mL), dried over Na_2SO_4 and filtered. The solvent was removed under reduced pressure. The residue was purified by flash chromatography (CH_2Cl_2/MeOH, 20:1) affording product **3** (2 g, 8.4 mmol, 79%) as a colourless oil; R*f*: 0.3 in CH_2Cl_2/MeOH, 20:1 (detected with phosphomolibdic acid). $[\alpha]_D^{20}$ = +102 (c 1.0 in $CHCl_3$); $[\alpha]_D^{20}$ = +96.1(lit.,[3] *c* 1.0 in $CHCl_3$). The spectroscopic data are in agreement with the reported data.[3]

2*S*,6*S*-(4-Boc-6-methoxymorpholin-2-yl)methanol (4).

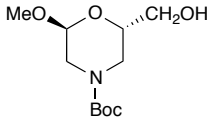

(+)-**4**

Operating in a round-bottom flask equipped with magnetic stirrer, compound **3** (1.5 g, 6.31 mmol) was dissolved in THF (150 mL). Boc_2O (1.4 g, 6.4 mmol) and Pd/C (1.7 g, 10% loading) were added to the solution. The suspension was stirred under H_2 (1 atmosphere) at 25 °C (R*f*: 0.28 in CH_2Cl_2/MeOH, 20:1; detected with phosphomolibdic acid). After 2 h, the mixture was filtered on Celite pad. The solvent was evaporated and the yellow oil was dissolved in CH_2Cl_2 (20 mL) washed with a 5% solution of $KHSO_4$ (20 mL) and a saturated solution of NaCl (20 mL). The organic layer was dried over Na_2SO_4, filtered and concentrated in vacuum. The purification of the crude by flash chromatography (CH_2Cl_2/MeOH, 20:1) afforded product **4** (1.4 mg, 5.4 mmol, 87%) as colorless oil. $[\alpha]_D^{20}$ = +2.17 (c 1.0 in $CHCl_3$); IR (NaCl) ν_{max}/cm^{-1} 3437, 1694, 1680; ^{1}H NMR (300 MHz, $CDCl_3$) δ 4.72 (br s, 1H), 3.90-4.01 (m, 2H), 3.71 (dd, *J* = 11.8, 3.6 Hz, 2H), 3.60 (dd, *J* = 11.8, 3.6 Hz, 1H), 3.37 (s, 3H), 3.03 (d, *J* = 13.2 Hz, 1H), 2.83 (br s, 1H), 2.08 (br s, 1H, exch.), 1.46 (s, 9H); ^{13}C NMR (75 MHz, $CDCl_3$) δ 155.6, 96.6, 80.5, 67.9, 63.8, 55.1, 46.9, 44.1, 28.7(x3); MS (ESI): *m/z* calcd for $[C_{11}H_{21}NO_5]$: 247.14; found: *m/z* 270.13 $[M+Na]^+$; Found: C, 53.21; H, 8.80; N, 5.44.Calcd for C, 53.43; H, 8.56; N, 5.66.

2*S*,6*S*-(4-Boc-6-methoxymorpholin-2-yl)carboxylic Acid (5).

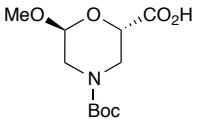

(+)-**5**

Operating in a round-bottom flask equipped with magnetic stirrer, compound **4** (1.2 g, 4.67 mmol) was dissolved in CH_2Cl_2 (17 mL) and the solution was cooled to 0 °C. TBABr (105 mg, 0.33 mmol), KBr (56 mg, 0.5 mmol), TEMPO (161 mg, 1.03 mmol), a solution of $NaHCO_3$ in water (1 M, 7.6 mL), NaClO (8.6 mL, 0.02 mmol), and brine (1 mL) were added. After 20 min., a saturated solution of $NaHCO_3$ (5.6 mL) was finally added and the mixture was stirred at 25 °C overnight (T.L.C.: CH_2Cl_2/MeOH, 20:1, detected with phosphomolibdic acid). The layers were separated. The aqueous phase was acidified with HCl (20 mL, 30%) and extracted with AcOEt (2 x 20 mL). The combined organic layers were dried over Na_2SO_4, filtered and concentrated under reduced pressure. The crude mixture was purified by flash chromatography (condizioni CH_2Cl_2/MeOH = 20/1) affording pure product **5** as colourless oil (1.0 g, 3.9 mmol, 83%). $[\alpha]_D^{20}$ = +103.16 (c 1 in MeOH); IR (NaCl) ν_{max}/cm^{-1} 2977, 1750, 1652; ^{1}H NMR (300 MHz, $CDCl_3$) δ 5.55 (brs, 1H, ech.), 4.81 (brs, 1H), 4.58 (dd, *J* = 10.4, 3.3 Hz, 1H), 4.30 (brs, 1H), 3.93 (brs, 1H), 3.44 (s, 3H), 3.24-2.80 (m, 2H), 1.49 (s,

9H); ^{13}C NMR (75 MHz, $CDCl_3$) δ 172.7, 155.2, 96.6, 81.2, 67.1, 55.7, 46.4, 44.6, 30.0 (x3); MS (ESI): *m/z* calcd for [$C_{11}H_{19}NO_6$]: 261.12; found: *m/z* 284.0 [M+Na]$^+$; Found C, 50.39; H, 7.65; N, 5.05. Calcd for C, 50.57; H, 7.33; N, 5.36.

General Procedure for the Coupling Condensation: Synthesis of Peptides 7a, 7b, 10 and 12. Operating in a round-bottom flask equipped with a magnetic stirrer and thermometer, acid compound **5** or dipeptide **9** or tripeptide **11** (1 equiv.) was dissolved in CH_2Cl_2 (3 mL). The solution was cooled to 0 °C. HOBt (1.1 equiv.) and EDC (1.1 equiv.) were added. After 1 h, amino compound dipeptide **6a** or **6b** or tripeptide **8a** or **8b** (1 equiv.) in CH_2Cl_2 (1 mL) was dropped, followed by the addition of DIEA (2 equiv.). The reaction mixture was stirred for 24 h at 25 °C. The organic layer was washed with a solution of $KHSO_4$ (5%, 5 mL), a saturated solution of $NaHCO_3$ (5 mL) and brine (5 mL). After drying over Na_2SO_4, the solvent was removed under reduced pressure. Purification of the crude product by silica gel flash chromatography (AcOEt/*n*hexane: **7a**, 1:1; **7b**,**10**, 2:1. CH_2Cl_2/MeOH: **12**, 20:1) afforded compound the corresponding peptide as a white solid.

***N*-Boc-(+)-β-Morph-*L*-Leu-*L*-Val-NH$_2$ (7a)**. TLC: AcOEt/*n*hexane, 1:1 (detected by phosphomolibdic acid). Yield: 95%; mp 162 °C (from AcOEt/*n*hexane; white solid); $[\alpha]_D^{20}$ = +52.56 (c 1 in MeOH); IR (NaCl) ν_{max}/cm^{-1} 1644, 1678; MS (ESI): *m/z* calcd for [$C_{22}H_{40}N_4O_7$]: 472.29; found: *m/z* 496.58 [M+Na]$^+$. For NMR data see Table TS1.

***N*-Boc-(+)-β-Morph-*L*-Leu-*L*-Val-OBn (7b).** TLC: CH_2Cl_2/MeOH, 20:1 (detected by phosphomolibdic acid). Purification by silica gel flash chromatography (AcOEt/*n*hexane, 2:1). Yield: 69%. Mp 50 °C; $[\alpha]_D^{20}$ = +5 (c 0.3 in MeOH); IR (NaCl) ν_{max}/cm^{-1} 3319, 1703,1656; MS (ESI): *m/z* calcd for [$C_{29}H_{45}N_3O_8$]: 563.32; found: *m/z* 586.56 [M+Na]$^+$. For NMR data see Table TS2.

***N*-Boc-*L*-Val-Gly-(+)-β-Morph-*L*-Leu-*L*-Val-NH$_2$ (10).** TLC: CH_2Cl_2/MeOH, 20:1 (detected by phosphomolibdic acid). Yield: 89%. Mp 145.2 °C (from AcOEt/*n*hexane, white solid); $[\alpha]_D^{20}$ = +40.12 (c 1 in MeOH). IR (NaCl) ν_{max}/cm^{-1} 1677, 1648; MS (ESI): *m/z* calcd for [$C_{29}H_{52}N_6O_9$]: 628.38; found: *m/z* 651.3 [M + Na]$^+$. For NMR data see Table TS3 (**10**) and TS4 (**10'**).

***N*-Boc-(+)-β-Morph-*L*-Leu-*L*-Val-(+)-β-Morph-L-Leu-L-Val-OBn (12).** TLC: AcOEt/*n*hexane, 2:1 (detected by phosphomolibdic acid). Purification by silica gel flash chromatography (AcOEt/*n*hexane, 2:1). Yield: 50%. Mp 96 °C, white solid; $[\alpha]_D^{20}$= +18 (c 0.3 in MeOH); IR (NaCl) ν_{max}/cm^{-1} 3414, 2961, 1740; MS (ESI): *m/z* calcd for [$C_{46}H_{74}N_6O_{13}$]: 918.53; found: *m/z* 942.60 [M+Na]$^+$. For NMR data see Table TS5 (**12**) and TS6 (**12'**).

General Procedure for *N*-termini Deprotection. Operating in a round-bottom flask equipped with magnetic stirrer, compound **7a** or **7b** (1 mmol) was dissolved in CH_2Cl_2 (15 mL). The solution was cooled to 0 °C and TFA (15 mL) was slowly dropped. The solution was stirred at 25 °C for 2 h. Compound **8a** workup: the solvent was removed under reducing pressure affording compound **8a**;

Compound **8b** workup: after 2h the solvent was removed. The crude mixture was dissolved in CH_2Cl_2 (15 mL), washed with a saturated solution of $NaHCO_3$ (10 mL) and dried over Na_2SO_4. The organic solution was concentrated under reduced pressure affording **8b**.

(+)-β-Morph-*L*-Leu-*L*-Val-NH$_2$ · CF$_3$CO$_2$H (8a). TLC: CH_2Cl_2/MeOH, 20:1 (detected by phosphomolibdic acid). The solid was used for the condensation reaction without further purification. Yield: 97%, white solid; IR (NaCl) ν_{max}/cm^{-1} 1674; 1544; ^{1}H NMR (CD_3OD, 300 MHz): δ 5.1 (s, 1H), 4.7 (dd, J = 11.7, J = 2,71), 4.25 (m, 1H), 4.1 (m, 1H), 3.45-3.6 (m, 4H), 3.05 (m, 1 H), 2.03 (m, 1H), 1.55 (m, 2H), 0.97-1.10 (m, 12 H); ^{13}C NMR (75 MHz, CD_3OD): δ 174.4, 172.7, 167.9, 94.3, 64.6, 58.2, 54.6, 51.6, 43.73, 40.25, 30.7, 29.3, 24.5, 21.9, 20.5, 18.3, 17.1 ppm; MS (ESI+): *m/z* calcd for [$C_{17}H_{32}N_4O_5$]: 372.32; found: *m/z* 473.29 [M+H]$^+$.

(+)-β-Morph-*L*-Leu-*L*-Val-OBn (8b). T.L.C.: CH_2Cl_2/MeOH, 40:1 (detected by phosphomolibdic acid). Purification on silica gel by flash chromatography (CH_2Cl_2/MeOH, 40:1) afforded compound **8b** as a colorless oil. Yield: 95%. $[\alpha]_D^{20}$ = -43 (c 0.6 in MeOH); IR (NaCl) ν_{max}/cm^{-1} 3307, 1740, 1658; ^{1}H NMR (300 MHz, $CDCl_3$) δ 7.25-7.3 (m, 5H), 6.97-6.89 (m, 2H), 5.12 (dd, J = 27.49-12.23 Hz), 4.58-4.47 (m, 3H), 4.24 (dd, J = 10.92-2.57 Hz, 1H), 3.33 (s, 3H), 3.27 (d, J = 2.34 Hz, 1H), 2.84 (m, 2H), 2.61 (dd, J = 13.19-11.35 Hz, 1H), 2.33 (s, 2H), 2.10-2.16 (m, 1H), 1.46-1.67 (m, 3H) 0.82-0.89 (m, 12H); ^{13}C NMR (75 MHz, $CDCl_3$) δ 171.7, 171.4, 170.0, 135.3, 128.5, 128.4, 128.3, 96.6, 68.6, 66.9, 57.2, 55.0, 50.9, 48.1, 47.8, 40.8, 31.0, 24.7, 22.8, 22.1, 18.9, 17.6; MS (ESI+): *m/z* calcd for [$C_{29}H_{45}N_3O_8$]: 463.27; found: *m/z* 464.33 [M+H]$^+$.

***N*-Boc-(+)-β-Morph-*L*-Leu-*L*-Val-OH (11).** Operating in a round-bottom flask equipped with a magnetic stirrer, compound **7b** (99 mg, 0.176 mmol) was dissolved in THF (3.5 mL) and Pd/C (100 mg, 10% loading) was added to the solution. The suspension was stirred under H_2 (1 atmosphere) at 25 °C for 2 h (T.L.C.: CH_2Cl_2/MeOH, 40:1; detected by phosphomolibdic acid). The catalyst was filtered over a Celite pad. The solvent was removed under reduced pressure and the obtained clear oil was dissolved in CH_2Cl_2 (20 mL) and washed with a saturated solution of $NaHCO_3$ (20 mL). The aqueous layer was then acidified with 37% HCl until pH 2. The product was extracted with CH_2Cl_2 (2 x 20 mL). The organic layer was concentrated under vacuum, affording compound **11** (77.6 mg, 0.164 mmol, 93%) as colourless oil. $[\alpha]_D^{20}$ = + 24 (c 1 in $CHCl_3$); IR (NaCl) ν_{max}/cm^{-1} 3272, 2917, 1702, 1685, 1632; ^{1}H NMR (300 MHz, $CDCl_3$): δ 7.25 (brs, 1H), 7.12 (d, J = 8.4 Hz, 1H), 4.71 (m, brs, 2H), 4.48 (m, 1H), 4.31 (m, 2H), 4.31 (m, 2H), 3.97 (brs, 1H), 3.33 (s, 3H), 3.09 (dd, J = 14.50-7.40 Hz, 1H), 2.93 (brs, 1H), 2.75 (brs, 1H), 2.17 (m, 1H), 1.55 (m, 3H), 1.44 (s, 9H), 0.89 (m, 12H); ^{13}C NMR (75 MHz, $CDCl_3$): δ 174.1, 171.6, 169.1, 155.1, 96.3, 80.7, 67.5, 57.4, 55.1, 51.1, 47.0, 45.6, 45.34, 41.0, 31.2, 29.7, 28.3, 24.7, 22.8, 22.3, 18.9, 17.6; MS (ESI): *m/z* calcd for [$C_{29}H_{45}N_3O_8$]: 473.27; found: *m/z* 496.42 [M+Na]$^+$.

2. NMR characterization of peptide *N*-Boc-(+)-β-Morph-*L*-Leu-*L*-Val-NH$_2$ (7a)

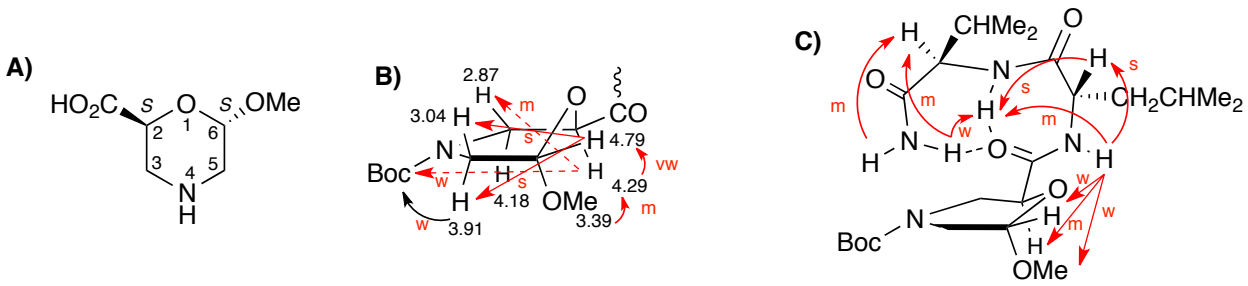

Figure S1. NOEs at (red arrows) and H-bond (dotted lines) for peptide **7a**. A) Stereochemistry of morpholino ring. B) NOEs of morpholino ring protons. C) NOEs between the different amino acids of peptide **7a**.

Table S1. ^{1}H, ^{13}C NMR (CD_3CN, 0.01 mM, 500 MHz) and NOE (900 ms) data for tripeptide **7a**

AA	atom	^{1}H NMR δ	Molteplicity *J* (Hz)	^{13}C NMR δ	Noesy
Morph-1	CO			169.1	
	H-2	H_{ax} 4.29	dd, *J* 10.8, 3.2	67.6	NH_{Leu} (m) H-6 (vw) H-3_{ax} (m) OMe (m) Boc (w)
	H-3	H_{ax} 2.87 H_{eq} 4.18	br overl	45.1	H-2 (m)
	H-5	H_{ax} 3.04 H_{eq} 3.91	br d, *J* 13.7	46.3	H-6 (s) ---------- H-6 (s) Boc (w)
	H-6	H_{eq} 4.79	br	96.7	H-5_{ax} (s) H-5_{eq} (s) OMe (s) NH_{Leu} (w)
	OMe	3.39	s	54.4	H-6 (s) H-2 (m) NH_{Leu} (w)
	Boc	1.46	s	27.3, 79.2	H-5_{eq} (w) H-2 (w)
	CO			[a]	
Leu-2	CO			171.7	
	CH	4.44	m	51.2	NH_{Leu} (s) NH_{Val} (s)
	CH_2 CH	1.62	m	40.6 24.8	CH_{Leu} (s)
	Me	0.94 0.97	overl	21.0 22.3	
	NH	7.20	d, *J* 8.1		OMe (w) H-2 (m) H_{Leu} (s) H-6 (w) NH_{Val} (m)
Val-3	CO			172.8	
	CH	4.18	overl	57.7	NH_2 (m)
	CH_{isopr}	2.09		30.6	H_{Val} (m)
	Me	0.90 0.94	d, *J* 9.9 overl	17.1	NH_{Val} (s) CH_{Val} (4.18, s)

	NH	6.83	d, *J* 8.5		Me_{Val} (0.90, vs) CH/CH_{2Leu} (s) CH_{Val}(m) CH_{Leu}(s) NH_2 (5.78,w; 6.29, vw) NH_{Leu} (m)
	NH_2	5.78 6.29	s s		CH_{Val}(4.18, m) CH_{Val}(2.09, w) NH_{Val}(w) ---------- CH_{Val}(m) $CH_{isoprVal}$(w) NH_{Val}(vw)

[a] Not assigned

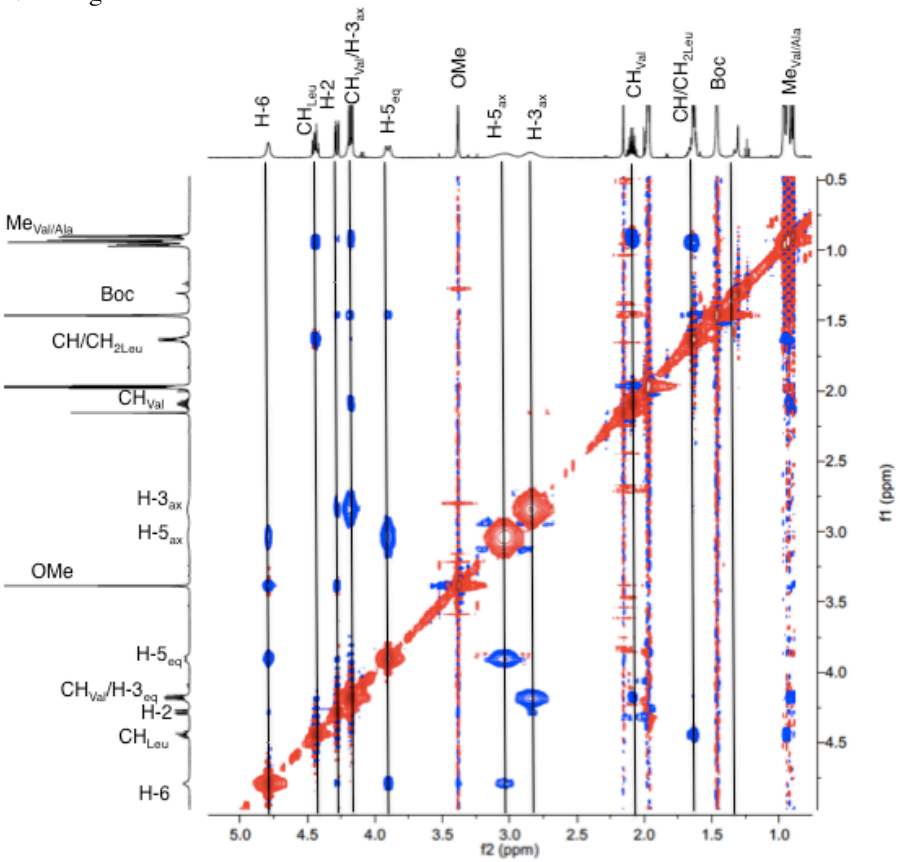

Figure S2. CH/CH region NOEs (CD_3CN, 0.01 mM, 500 MHz, 900 ms) for compound **7a**

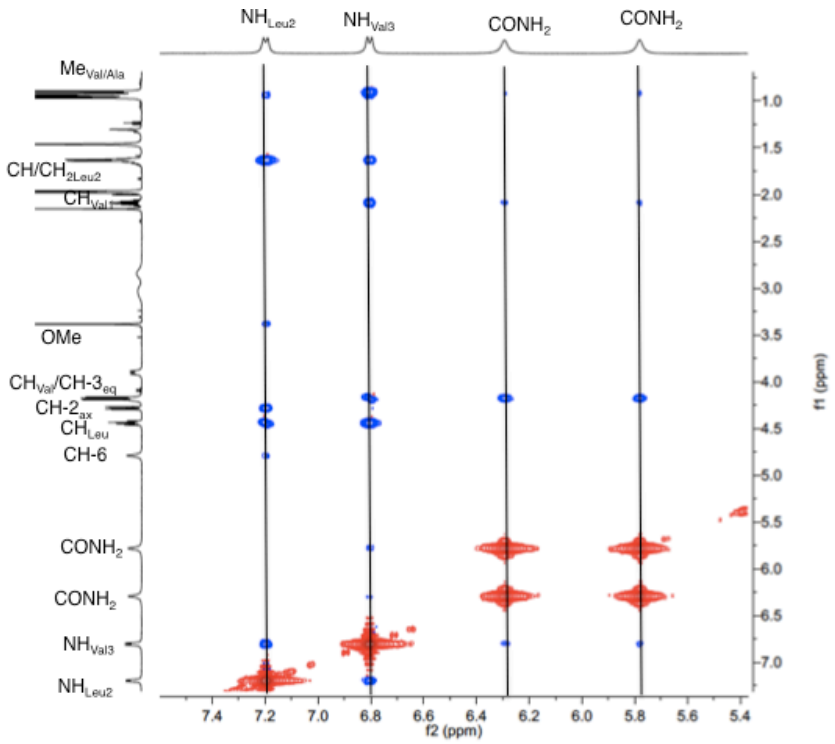

Figure S3. NH/NH and NH/CH NOE regions (CD_3CN, 0.01 mM, 500 MHz, 900 ms) for compound **7a**

3. NMR characterization of *N*-Boc-(+)-β-Morph-*L*-Leu-*L*-Val-OBn (7b)

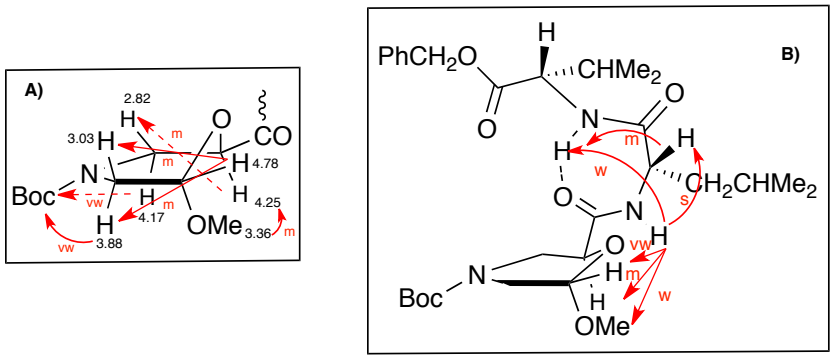

Figure S4. NOEs (red arrows) and H-bond (dotted lines) for peptide **7b**. A) NOEs of morpholino ring protons. B) NOEs between the different amino acids.

Table S2. ^1H, ^{13}C NMR (CD_3CN, 0.02 mM, 500 MHz) and NOE (1.1 s) data for tripeptide **7b**

AA	**atom**	^1H NMR δ	Molteplicity J (Hz)	^{13}C NMR δ	Noesy
Morph-1	CO			168.8 [a]	
	H-2	4.25	dd, J 10.9 J 3.2	67.5	NH_{Leu} (w) H-3_{ax} (m) OMe (w)
	H-3	H_{ax} 2.82 H_{eq} 4.17	br d, J 13.1	45.6	H-2 (m) H-3_{eq} (s) ---------- H-3_{ax} (s) Boc (vw)
	H-5	H_{ax} 3.03	br	45.9	H-6 (m) H-5_{eq} (vs)

		H_{eq} 3.88	d, *J* 14.4		---------- H-6 (m) $H\text{-}5_{ax}$ (vs) Boc (vw)
	H-6	4.78	br	96.3	$H\text{-}5_{ax}$ (m) $H\text{-}5_{eq}$ (m) OMe (m) NH_{Leu} (vw)
	OMe	3.36	s	54.4	H-6 (m) NH_{Leu} (w)
	Boc	1.46	s	79.7 27.5	$H\text{-}5_{eq}$ (w) $H\text{-}3_{eq}$ (w)
	CO			154.2 [a]	
Leu-2	CO			171.2 [a]	
	CH	4.47	m	50.9	NH_{Leu} (s) CH/CH_2 (s) NH_{Val} (s) Me (m)
	CH/CH_2	1.57	overl	40.9 24.5	CH_{Leu} (s) Me (vs) NH_{Leu}(s)
	Me	0.90 0.91	overl	21.1 22.3	
	NH	7.14	d, *J* 8.4		OMe (w) CH/CH_{2Leu} (s) H-2 (m) H-6 (vw) CH_{Leu} (s) NH_{Val} (w)
Val-3	CO			171.9[a]	
	CH	4.36	dd, *J* 5.7 *J* 8.3	57.6	Me (s) CH_{Val} (m) NH_{Val} (m)
	CH_{isopr}	2.15	m	30.4	Me (s) CH_{Val} (m)
	Me	0.89 0.93	overlapped	17.2 18.3	NH_{Val} (s) CH_{Val} (s)
	NH	6.89	d, *J* 7.9		Me (0.91, s) CH_{2Leu} (w) CH_{Val} (m) CH_{isopr}Val (w) CH_{Leu} (s) NH_{Leu} (w)
	OCH_2	5.14	dd, *J* 12.4 *J* 17.5	66.5	CH_{Val} (vw) Bn (m)
	Bn	7.41-7.36	m	128.2 128.5 129.6 136.0	CH_{2Leu} (vw) OCH_2 (m)

[a] Tentatively assigned

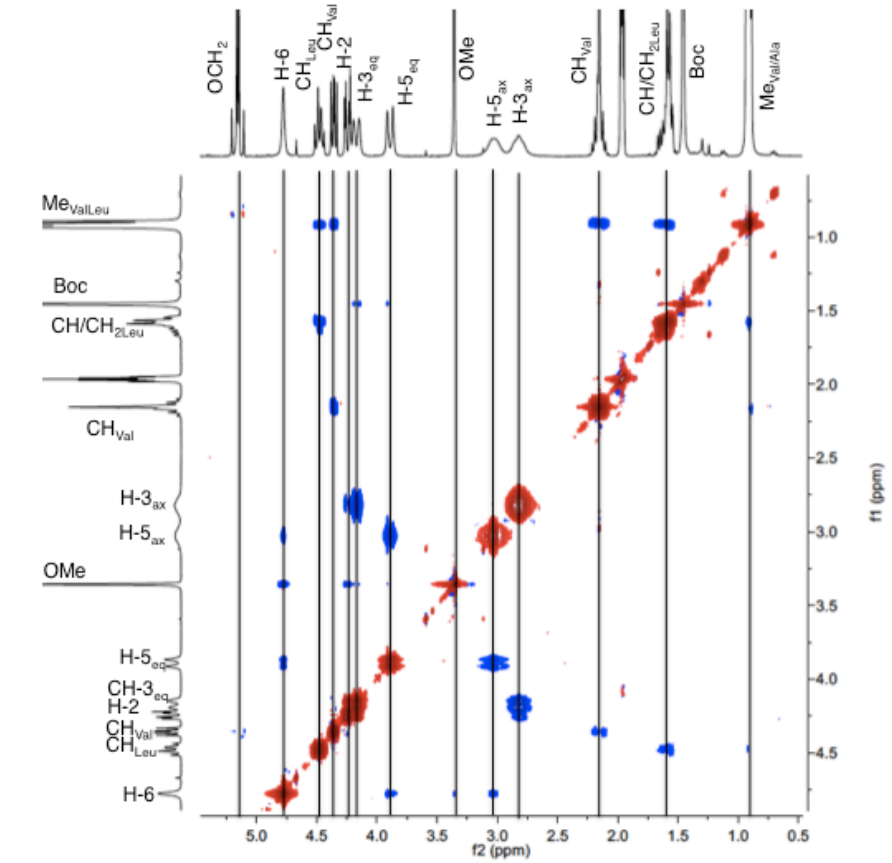

Figure S5. CH/CH NOE region (CD_3CN, 0.02 mM, 500 MHz, ms 1.1 s) for compound **7b**

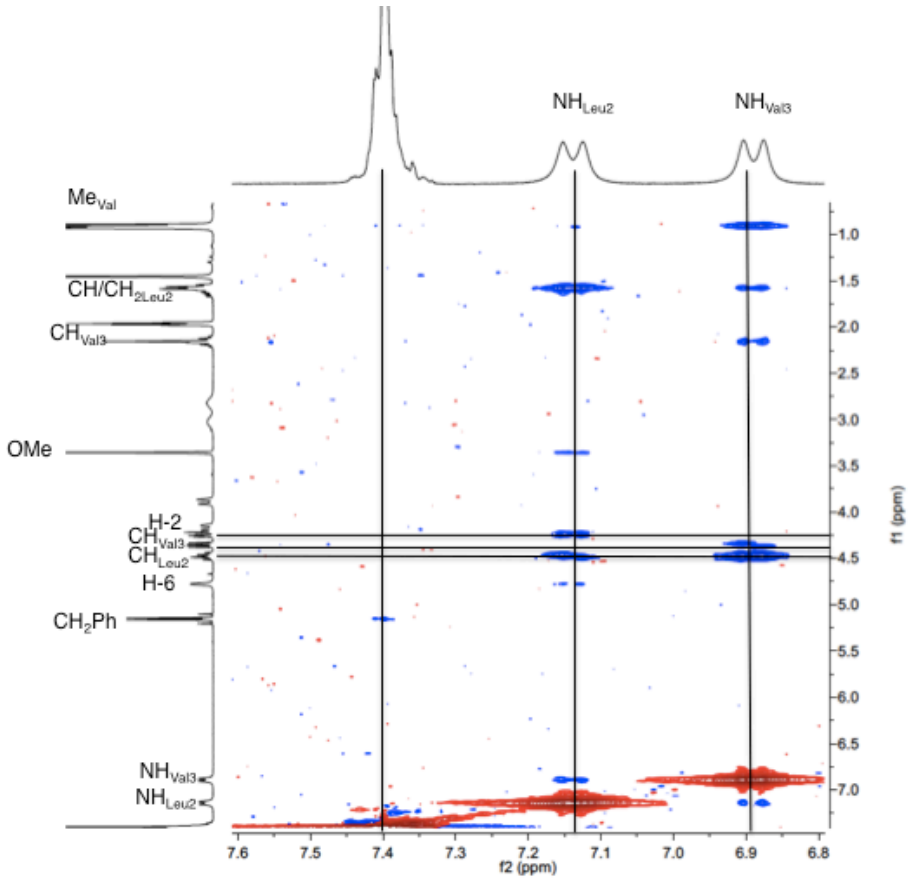

Figure S6. NH/NH and NH/CH NOE regions (CD_3CN, 0.02 mM, 500 MHz, ms 1.1 s) for compound **7b**

4. NMR characterization of *N*-Boc-*L*-Val-Gly-(+)-β-Morph-*L*-Leu-*L*-Val-NH$_2$ (10/10')

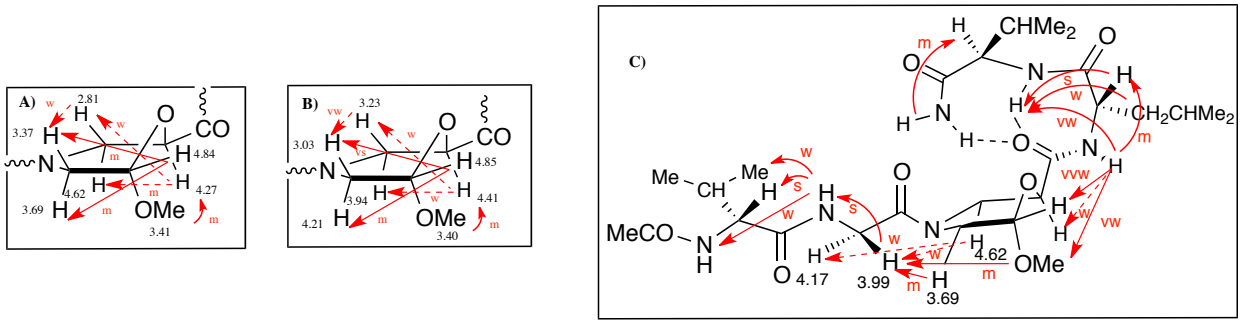

Figure S7. NOEs (red arrows) and H-bond (dotted lines) for peptide **10**. A) NOEs protons of morpholino ring in isomer **10***. B) NOEs protons of morpholino ring in isomer **10'°**. B) NOEs between the different amino acids.

Tables S3/S4. ^{1}H, ^{13}C NMR (CD_3CN, 0.009 mM, 500 MHz) and NOE (500 ms) data for pentapeptide **10/10'**

Table S3. Isomer **10**

AA	**atom**	^{1}H δ	Molteplicity *J* (Hz)	^{13}C δ	Noesy
Val-1	CO			171.6	
	CH	3.96	overl.	59.7	NH_{Gly} (s) NH_{Val1} (m)
	CH	2.13-2.05		30.6	
	Me	0.95 0.90	d, *J* 6.0	18.6 16.9	NH_{Gly} (s)
	NH	5.53	br		NH_{Gly} (w) CH_{Val1} (m)
	CO			[a]162.7	
	Me	1.44		27.6	CH_{Val1} (w)
Gly-2	CO			167.4	
	CH_2	3.99 4.17	overl.	40.6	NH_{Gly} (s) H_{eq}-3 (w) H_{eq}-5 (m) OMe (3.41, m) --- H_{eq}-3 (w)
	NH	6.98	br		CH_{Gly} (s) NH_{Val1} (w) CH_{Val1} (s) Me (0.95, w) $CH_{isoprVal1}$ (w)
Morf	CO			168.7	
	CH-2	4.27	dd, *J* 11.0, 3.3	67.8	NH_{Leu4} (w) H-3 (4.62 m, 2.81 w) OMe (m)
	CH_2-3	H_{ax} 2.81 H_{eq} 4.62	dd, *J* 13.3, 11.0 d, *J* 13.3	43.7	H-5_{ax} (w) H-2 (w) H-3 (s) --- H-2 (m) CH_{2Gly} (w) H-3_{ax} (s)
	CH_2-5	H_{ax} 3.37 H_{eq} 3.69	overl d, *J* 14.0	47.5	H-3_{ax} (w) H-5_{eq} (s) H-6 (m) --- CH_{Gly} (3.99, m)

					H-6 (m) H-5$_{ax}$(s)
	CH-6	4.84	br	95.3	OMe (m) H-5 (3.69 m, 3.37 m)
	OMe	3.41		54.6	H-2 (m) H-6 (s) CH$_{Gly}$ (3.99, m)
Leu-4	CO			171.7	
	CH	4.44		51.4	NH$_{Val5}$(s)
	CH$_2$ CH	1.68-1.62	m	40.4 24.6	NH$_{Val5}$(w) NH$_{Leu}$ (m)
	Me	0.96 0.94	overl.	22.3 21.0	
	NH	7.20	d, *J* 8.1		CH$_{Leu}$(m) H-2 (w) H-6 (vvw) OMe (vw) NH$_{Val5}$(vw)
Val-5	CO			172.9	
	CH	4.18	m	57.7	NH$_2$(w) NH$_{Val5}$ (m)
	CH	2.13-2.05	m	30.6	
	Me	0.93 0.90	d, *J* 7.3	21.0 16.8	
	NH	6.83	d, *J* 8.6		CH/CH$_{2Leu}$ (w) CH$_{Leu}$ (s) CH$_{Val5}$ (m) NH$_{Leu4}$ (vw)
	NH$_2$	5.79 6.31	s s		CH$_{Val5}$(w)

[a]Tentatively assigned

Table TS4. Isomer **10'**

AA	**atom**	^{1}H δ	Molteplicity *J* (Hz)	^{13}C δ	Noesy
Val-1	CO			171.5	
	CH	3.96	overl	59.7	NH$_{Gly}$ (vs) NH$_{Val1}$ (m)
	CH	2.13-2.05		30.61	
	Me	0.95 0.90	d, *J* 6.0	18.7 16.9	
	NH	5.53	overl		NH$_{Gly}$ (m) CH$_{Val1}$ (m)
	CO			162.7[a]	
	Me	1.44	overl	27.6	
Gly-2	CO			167.9	
	CH$_2$	4.02	overl	40.5	
	NH	6.95	overl		
Morf	CO			[b]	
	H-2	4.41	dd, *J* 10.6, 6.4	67.9	H-3 (3.23,w; 3.94,m) MeO (m) NH$_{Leu}$ (vw)
	H-3	H$_{ax}$ 3.23	m	45.5	H-2 (w) H-5$_{ax}$ (vw)

		H_{eq} 3.94	overl		H-3$_{eq}$ (s) ---------- H-2 (w) H-3$_{ax}$(s)
	H-5	H_{ax} 3.03 H_{eq} 4.21	dd *J* 13.7, 2.6 overl	44.1	H-6 (m) H-3$_{ax}$ (vw) H-5$_{eq}$(s) ---------- H-5$_{ax}$(s) H-6 (4.85, m)
	H-6	4.85	brs	96.4	OMe (m) H-5 (3.03 m, 4.21 m)
	OMe	3.40		54.5	H-2 (m)
Leu-4	CO			171.6	
	CH	4.45		51.6	NH_{Val5}(s) NH_{Leu4} (s)
	$CHCH_2$	1.68-1.62	m	40.5 24.6	
	Me	0.96 0.94	overl	22.3 21.0	
	NH	7.29	d, *J* 8.2		CH_{Leu4} (m) NH_{Val5}(vw)
Val-5	CO			172.9	
	CH	4.19	m	57.6	NH_2 (w) NH_{Val5} (m)
	CH_{isopr}	2.13-2.05	m	30.7	
	Me	0.94 0.91		[a]21.0 19.9	
	NH	6.88	d, *J* 7.9		CH/CH_{2Leu} (w) CH_{Leu} (s) CH_{Val5} (m) NH_{Leu4}(vw)
	NH_2	5.87 6.35	s		CH_{Val5}(w)

[a]Tentatively assigned; [b]Not assigned

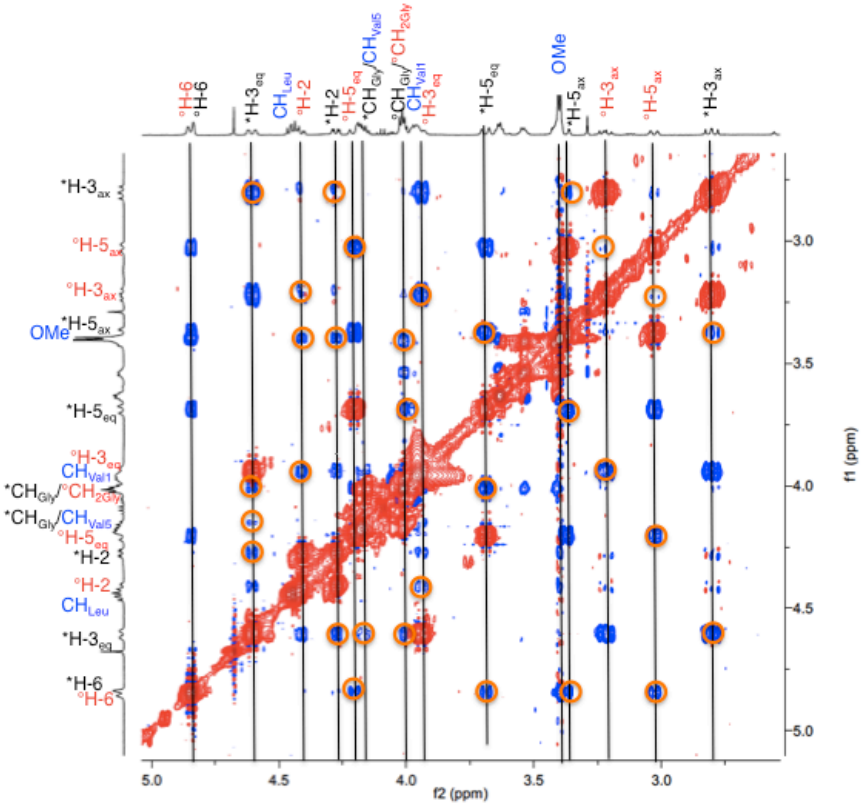

Figure S8. CH/CH region NOEs (CD_3CN, 0.009 mM, 500 MHz) for pentapeptide **10/10'. 10**: *(black); **10'**: °(red). Blu: overlapper signals for */°.

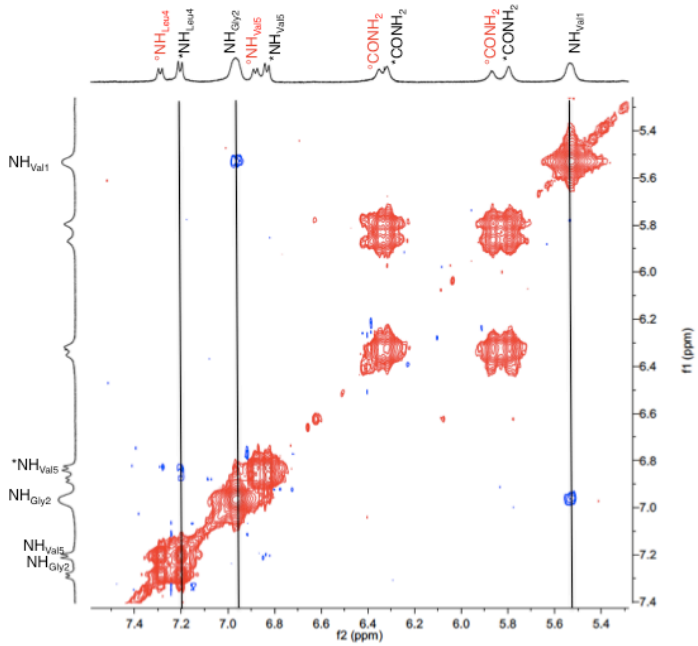

Figure S9. NH/NH region NOEs (CD_3CN, 0.009 mM, 500 MHz) for pentapeptide **10/10'**. **10**: *(black); **10'**: °(red). Blu: overlapper signals for */°.

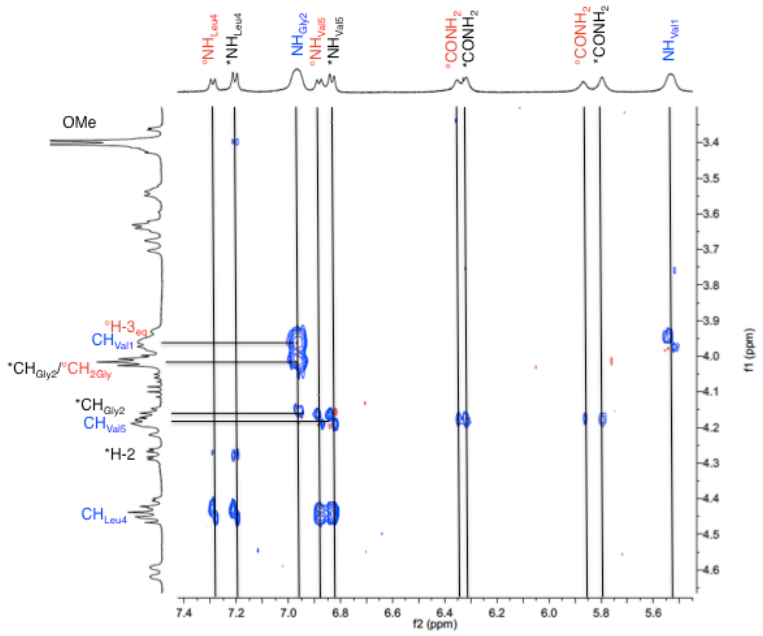

Figure S10. CH/NH region NOEs (CD_3CN, 0.009 mM, 500 MHz) for pentapeptide **10/10'**. **10**: *(black); **10'**: °(red). Blu: overlapper signals for */°.

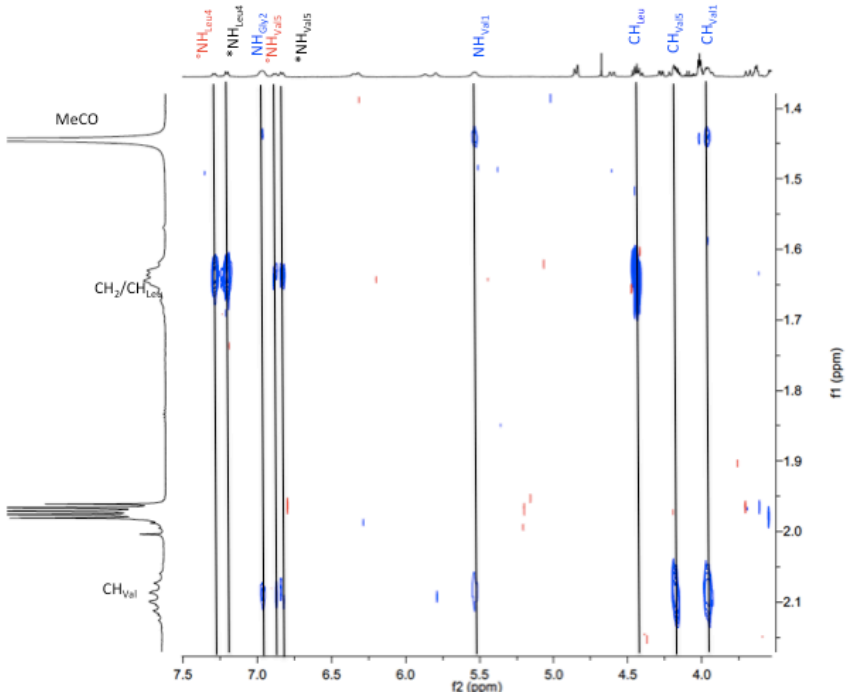

Figure S11. Me and CH/NH region NOEs (CD_3CN, 0.009 mM, 500 MHz) for pentapeptide **10/10'**. **10**: *(black); **10'**: °(red). Blu: overlapper signals for */°.

5. NMR characterization of N-Boc-(+)-β-Morph-L-Leu-L-Val-(+)-β-Morph-L-Leu-L-Val-OBn 12/12'

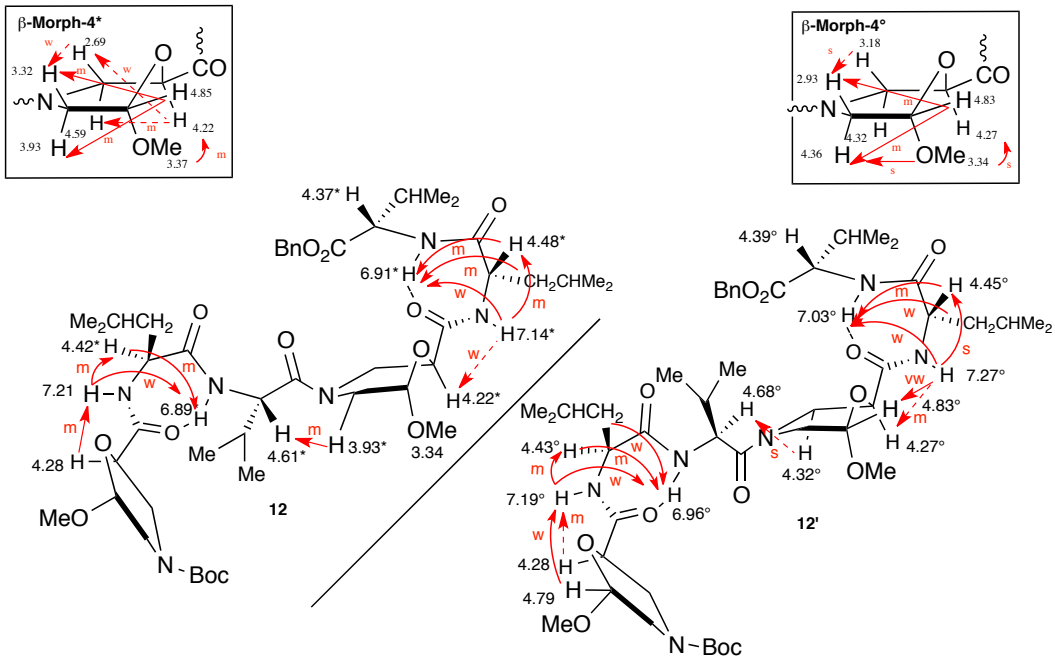

Figure S12. NOEs (red arrows) and H-bond (dotted lines) for peptide **12**. A) NOEs protons of of morpholino ring*. B) NOEs protons of of morpholino ring°. B) NOEs between the different amino acids.

Tables S5/S6. ^{1}H, ^{13}C NMR (CD_3CN, 0.009 mM, 500 MHz,) and NOEs (500 ms) data for **12/12'**.

Table TS5. Isomer **12**

AA	Atom	^{1}H δ	Molteplicity *J* (Hz)	^{13}C δ	Noesy
Morf-1	CO			[a]	
	CH-2	4.28	overl	overl[b]	OMe (s) NH_{Leu2}(m)
	CH_2-3	H_{ax} 2.83 H_{eq} 4.19	br	43.46	H_{eq}-3_{Morph4}(vvs) --- H_{ax}-3_{Morph4}(vvs) Boc(w)
	CH_2-5	H_{ax} 3.05 H_{eq}3.89	br br	48.4	H_{eq}-5_{Morph4}(vvs) H-6_{Morph4}(w) --- H_{ax}-5_{Morph4}(vvs) H-6_{Morph4}(s) Boc (w)
	CH-6	4.79	br	96.28	OMe (s) H-5_{Morph4}(3.89,s; 3.05,w)
	OMe	3.39		54.46	H-2_{Morph4}(s) H-6_{Morph4}(s)
	BOC	1.46		27.5, 79.7	H_{eq}-3_{Morph4}(w) H_{eq}-5_{Morph4}(w)
Leu-2	CO			171.45	
	CH	4.43	m	51.6	NH_{Val3}(m) NH_{Leu2}(m) Me_{Leu2}(vs) CH_{2Leu2}(vs)
	CH_2	1.64-1.56	overl	40.9	

	CH			[c]	
	Me	0.87[d]	overl	[e]	
	NH	7.21	d *J* 8.1		NH_{Val3}(w) CH_{Leu2}(m) H-2_{Morph1}(m)
Val-3	CO			170.41	
	CH	4.61	m	53.2	H_{eq}-5_{Morph4}(m) Me_{Val3}(0.87, s)
	CH	2.27-2.20	m	30.4	NH_{Val3}(m)
	Me	0.87[d]		[e]	NH_{Val3}(vs)
	NH	6.89	br		CH_{Leu2}(4.43,m) NH_{Leu2}(w) CH_{Val3}(m) Me_{Val3}(0.87,vs) $Me_{Val3??}$(0.92,vs)
Morf-4	CO			168.45	
	CH-2	4.22	dd *J* 11.0, 3.3	67.9	NH_{Leu5}(w) H-3_{Morph4}(4.59 s, 2.69 w) OMe (m)
	CH_2-3	H_{ax} 2.69 H_{eq} 4.59	dd *J* 13.3, 11.0 d *J* 13.3	43.5	H_{ax}-5_{Morph4}(w) H-2_{Morph4}(w), H_{eq} -3_{Morph4} (s) ---------- H_{ax}-3_{Morph4}(2.69,s)
	CH_2-5	H_{ax} 3.32 H_{eq} 3.93	overl d *J* 14.0	47.97	H_{ax}-3_{Morph4}(w) H-6_{Morph4}(m) H_{eq}-5_{Morph4}(s) ---------- H_{ax}-5_{Morph4}(s) H-6_{Morph4}(m) CH_{Val3}(m)
	CH-6	4.85	brs	95.8	OMe (s) H-5_{Morph4}(m)
	OMe	3.37	~~s~~	54.51	H-6_{Morph4}(s) H-2_{Morph4}(m)
Leu-5	CO			171.92	
	CH	4.49	m	51.9	NH_{Val6}(m) CH_{2Leu5}(s) Me_{Leu5}(0.93,s) NH_{Leu5}(m)
	CH_2 CH	1.68-1.62	overl	40.9 [b]	NH_{Val6}(m) NH_{Leu5}(s) CH_{Leu5}(s)
	Me	0.93[d]	overl	[e]	NH_{Leu5}(vw)
	NH	7.14	d *J* 8.1		Me_{Leu5}(0.93, vw) CH_{2Leu5}(1.59,s) CH_{Leu5}(4.49,m) H-2_{Morph4} (w) NH_{Val6}(w)
Val-6	CO			171.25	
	CH	4.37	m	57.66	CH_{Val6}(2.18,vs) Me_{Val6}(0.92,vs) NH_{Val6}(m)
	CH	2.20-1.12	m	30.3	CH_{Val6} (vs)
	Me	0.92, 0.87	overl	[e]	NH_{Val6}(vs)
	NH	6.91	d, *J* 8.6		CH_{2Leu5}(1.60,m) CH_{Leu5}(4.49,m)

					NH_{Leu5}(w) CH_{Val6}(2.18w) CH_{Val6}(4.37,m) Me(0.93, vs)
	OBn	Ph 7.42-7.40 CH_2 5.16	m dd *J* 12.5	138.1, 128.5, 128.3, 128.2 66.5	OCH_2(m) Me (0.92m) Me (0.87,w) ----------

[a]169.1 or 168.9; [b]67.6-67.3 region; [c]CH: 27.5 or 24.5; [d]Only certain Me were assigned; [e]22.3-16.4 region.

Table S6. Isomer **12'**

AA	**Atom**	^{1}H δ	Molteplicity *J* (Hz)	^{13}C δ	Noesy
Morf-1	CO			[a]	
	CH-2	4.28	overl	68 (overl)	OMe (s) NH_{Leu2}(m)
	CH_2-3	H_{ax} 2.83 H_{eq} 4.19	br	45.1	H_{eq}-3_{Mosphd}(vvs) --------- H_{ax}-3_{Mosphd}(vvs) Boc(w)
	CH_2-5	H_{ax} 3.05 H_{eq} 3.89	br br	Not detect	H_{eq}-5_{Mosphd}(vvs) H-6_{Morpb4}(w) --------- H_{ax}-5_{Mosphd}(vvs) H-6_{Morpb4}(s) Boc(w)
	CH-6	4.79	br	96.3	OMe(s), NH_{Leu2}(w) H-5_{Morpb4}(3.89,s; 3.05,w)
	OMe	3.39	s	54.47	H-2_{Morpb4}(s) H-6_{Morpb4}(s)
	BOC	1.46			H_{eq}-3_{Mosphd}(w) H_{eq}-5_{Mosphd}(w)
Leu-2	CO			171.63	
	CH	4.43	m	51.9	NH_{Val3}(m) NH_{Leu2}(m) Me_{Leu2}(vs) CH_{2Leu2}(vs)
	CH_2 CH	1.64-1.56	m	40.9 [b]	NH_{Val3}(w) CH_{Leu2}(vs)
	Me	0.93[c]	overl	[d]	CH_{Leu2}(s)
	NH	7.19	d *J* 8.1		CH_{Leu2}(m) CH_{2Leu2}(s) H-2_{Morph1}(m) H-6_{Morph1}(w) NH_{Val3}(w)
Val-3	CO			169.86	
	CH	4.68	m	53.4	Me (0.87,s) H-3_{Morpb4}(4.32,s) NH_{Leu2}(m)
	CH	2.23-2.14	m	30.5	NH_{Val3}(m)
	Me	0.87[c]	overl	[d]	NH_{Val3}(w)
	NH	6.96	brs		CH_{Leu2}(m) CH_{2Leu2}(1.62,w) NH_{Leu2}(w) CH_{Val3}(m)

					Me_{Val3}(vs) CH_{Val3}(2.07,w)
Morf-4	CO			168.35	
	CH-2	4.27	dd *J* 10.6, 6.4	68.0	MeO (s) NH_{Leu5}(m)
	CH_2-3	H_{ax} 3.18 H_{eq} 4.32	m Overl	47.2	H_{eq}-3_{Morph4}(s) H_{ax}-5_{Morph4}(s) ---------- H_{ax}-3_{Morph4}(s) CH_{Val3}(s)
	CH-5	H_{ax} 2.93 H_{eq} 4.36	dd *J* 13.7, 2.6 overl	43.8	H-6_{Morph4}(m) H_{eq}-5_{Morph4}(s) H_{ax}-3_{Morph4}(s) ---------- H_{ax}-5_{Morph4}(s) H-6_{Morph4}(m) OMe(s)
	CH-6	4.83	br	96.5	OMe(s) H-5_{Morph4}(2.93m, 4.36 s) NH_{Leu5}(vw)
	OMe	3.34		54.5	H-2_{Morph4}(s) H_{eq}-5_{Morph4}(s) H-6_{Morph4}(s)
Leu-5	CO			171.98	
	CH	4.45		51.4	NH_{Val6}(m) NH_{Leu5}(m) Me_{Leu5}(s) $CH_{2\,Leu5}$(vs)
	CH_2 CH	1.68-1.62	m	40.9 [b]	NH_{Val6}(w)
	Me	0.96 0.93	overl	[d]	
	NH	7.27	d *J* 8.2		NH_{Val6}(w) CH_{2Leu5}(1.61, s) CH_{Leu5}(4.45, m) H-2_{Morph4} (4.27,m) H-6_{Morph4} (4.83,vw)
Val-6	CO			171.33	
	CH	4.39	m	57.6	NH_{Val6}(m) Me_{Val6}(s)
	CH	2.13-2.05	m	30.3	NH_{Val6}(m)
	Me	0.92[c]	overl	[d]	NH_{Val6}(vs)
	NH	7.03	d, *J* 7.9		CH_{Val6}(4.39, m) CH_{Val6}(2.18, m) Me_{Val6}(0.92, vs) NH_{Leu5}(w) CH_{Leu5}(m) CH_{2Leu5}(1.60, w)
	OBn	Ph 7.42-7.40 CH_2 5.16	m dd *J* 12.5	138.1, 128.5, 128.3, 128.2 66.5	OCH_2(m) Me (0.92m) Me (0.87,w)

[a]169.1 or 168.9; [b]CH: 27.5 or 24.5; [d]Only certain Me were assigned; [e]22.3-16.4 region.

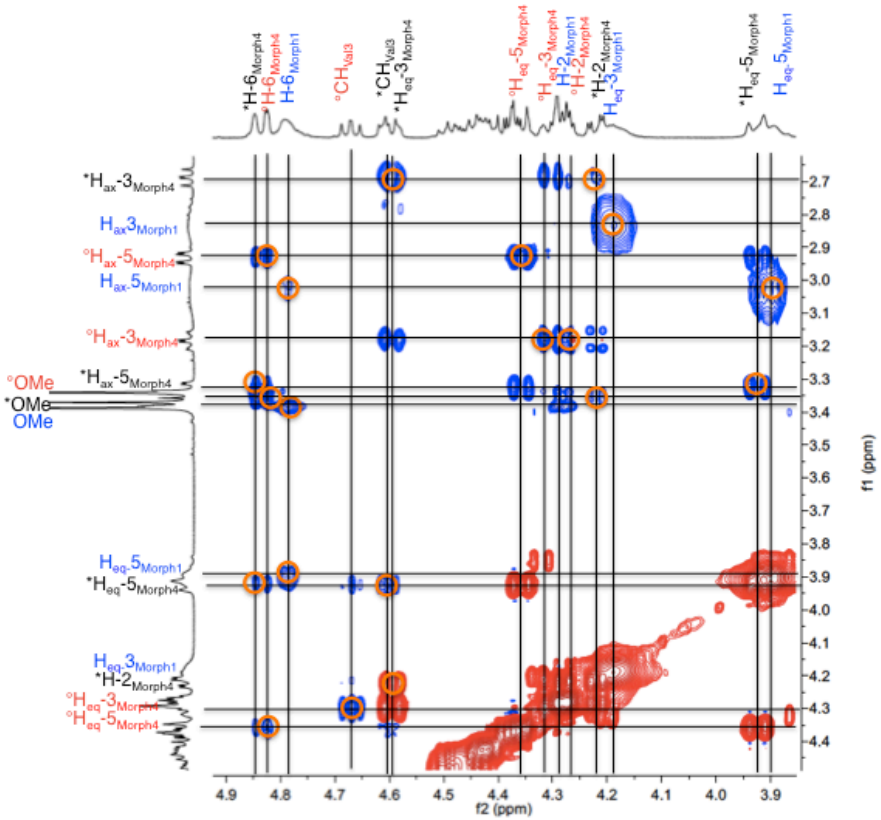

Figure S13. CH/CH region NOEs (CD$_3$CN, 0.009 mM, 500 MHz) for pentapeptide **10/10'. 10**: *(black); **10'**: °(red). Blu: overlapper signals for */°.

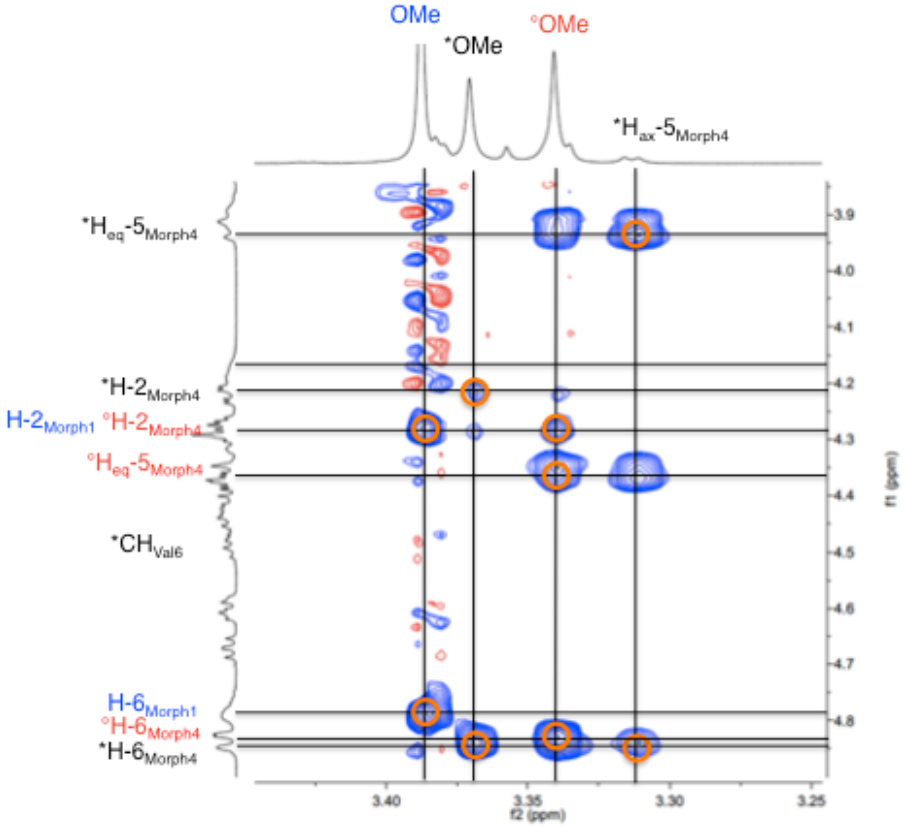

Figure S14. Zoom of the NOEs CH/CH region (CD$_3$CN, 0.009 mM, 500 MHz) for pentapeptide **10/10'. 10**: *(black); **10'**: °(red). Blu: overlapper signals for */°.

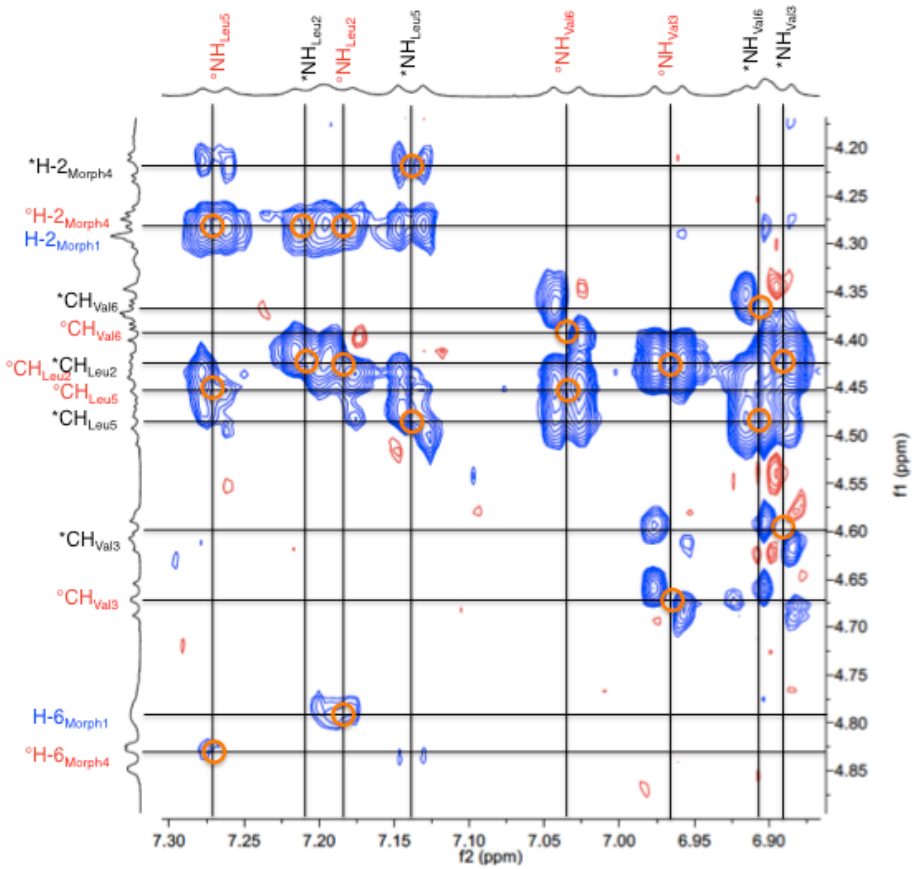

Figure S15. CH/NH region NOEs (CD_3CN, 0.009 mM, 500 MHz) for pentapeptide **10/10'. 10**: *(black); **10'**: °(red). Blu: overlapper signals for */°.

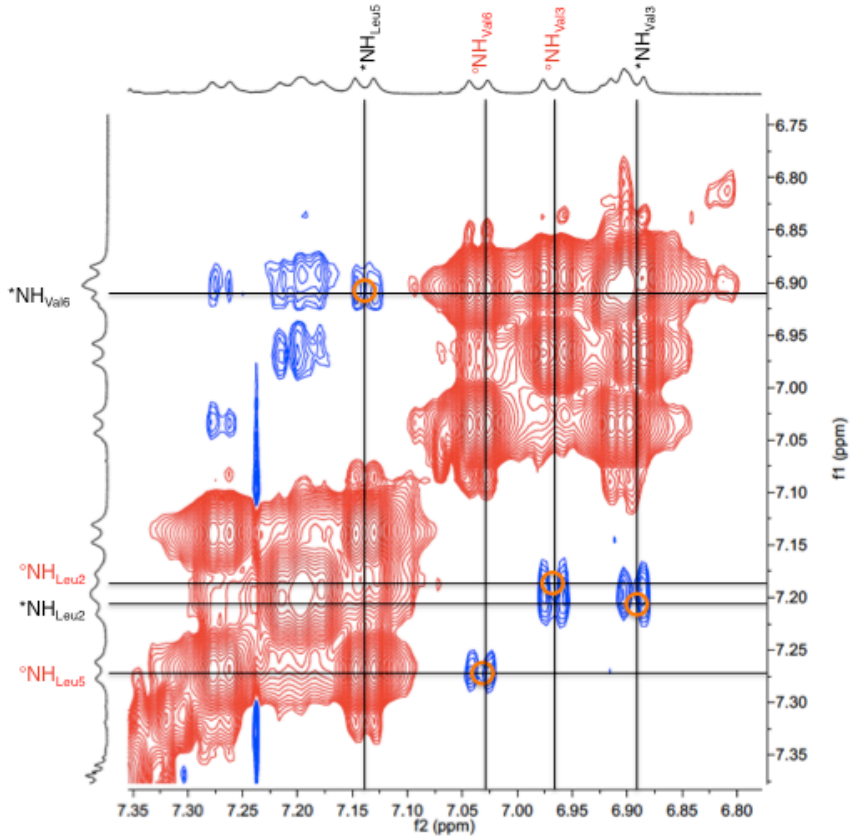

Figure S16. NH/NH region NOEs (CD_3CN, 0.009 mM, 500 MHz) for pentapeptide **10/10'. 10**: *(black); **10'**: °(red). Blu: overlapper signals for */°.

6. Computational studies

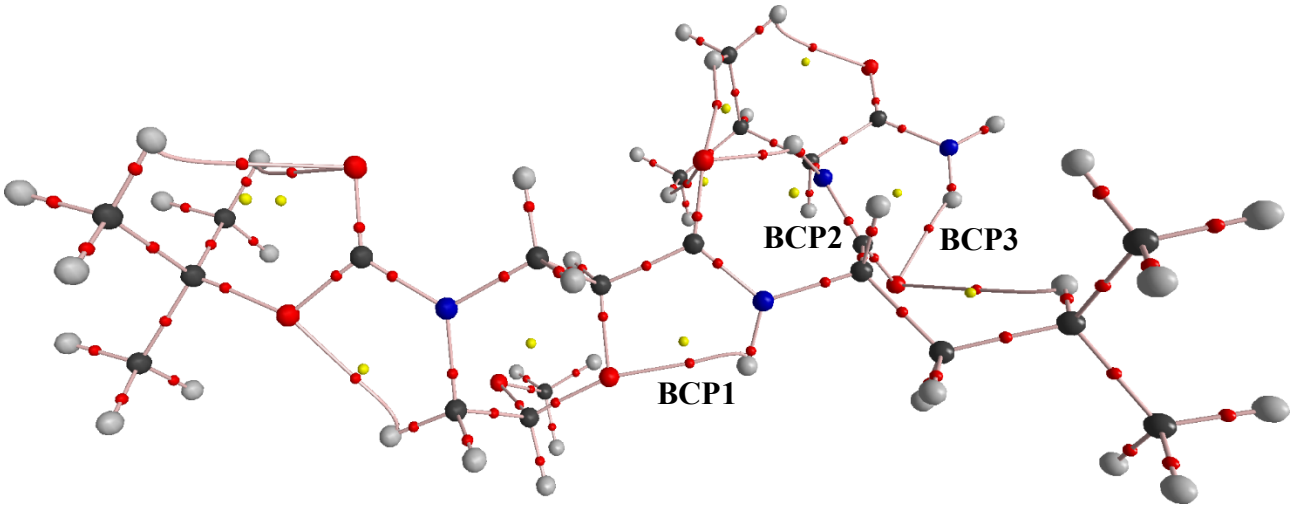

Figure S17. Molecular graph from the QTAIM analysis of cluster1 geometry optimized at the mPW1B95/6-31+G(d,p) level of theory. Bond critical points (BCP) and ring critical points are depicted as red and yellow dots, respectively, while bond paths are represented as pink lines. Relevant parameters for selected BCPs (including x,y,z Cartesian coordinates) are: BCP1 (0.213860, 2.832669, 1.850284): $\rho(r_c)$ = 0.0213 a.u.; $\nabla^2(r_c) = -0.0233$; BCP2 (3.566037, -1.347934, -1.939387): $\rho(r_c)$ = 0.0208 a.u.; $\nabla^2(r_c) = -0.0158$; BCP3 (9.918951, -0.448641, 1.455184): $\rho(r_c)$ = 0.0216 a.u.; $\nabla^2(r_c) = -0.0164$

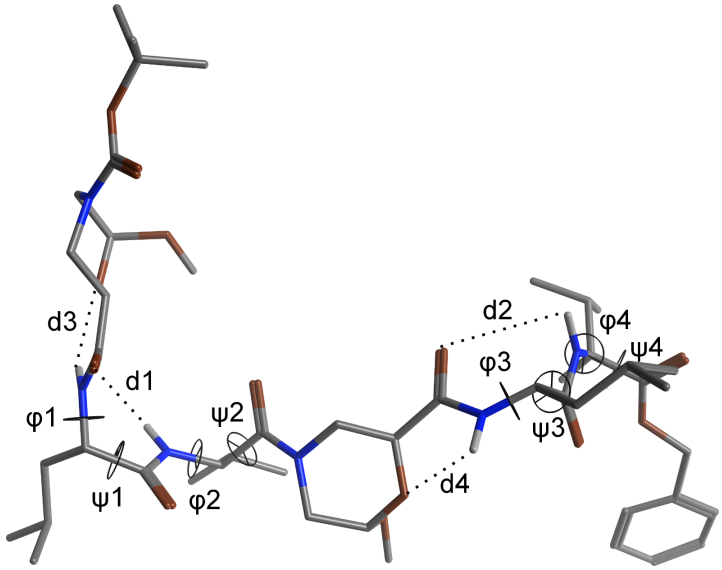

Figure S18. Most representative conformation of cluster2 (pop. = 29.2%) obtained from the analysis of the 750-1000 ns segment of the aMD trajectory of *E*-**12**, conducted in explicit CH_3CN using the ff14SB force field. Selected geometrical parameters are: d1 = 4.4 ± 0.8; d2 = 3.3 ± 0.8; d3 = 2.2 ± 0.5; d4 = 2.6 ± 0.3; φ1 = -74.2 ± 31.4; ψ1 = -51.6 ± 25.6; φ2 = -78.3 ± 39.6; ψ2 = 114.5 ± 23.1; φ3 = -68.2 ± 26.2; ψ3 = 121.6 ± 67.6; φ4 = -69.9 ± 31.1; ψ4 = 119.9 ± 59.2. Distances are reported in Å, dihedrals in deg. The values are taken from the non-minimized most representative conformation, while intervals are the mean deviations of the whole cluster population from the centroid.

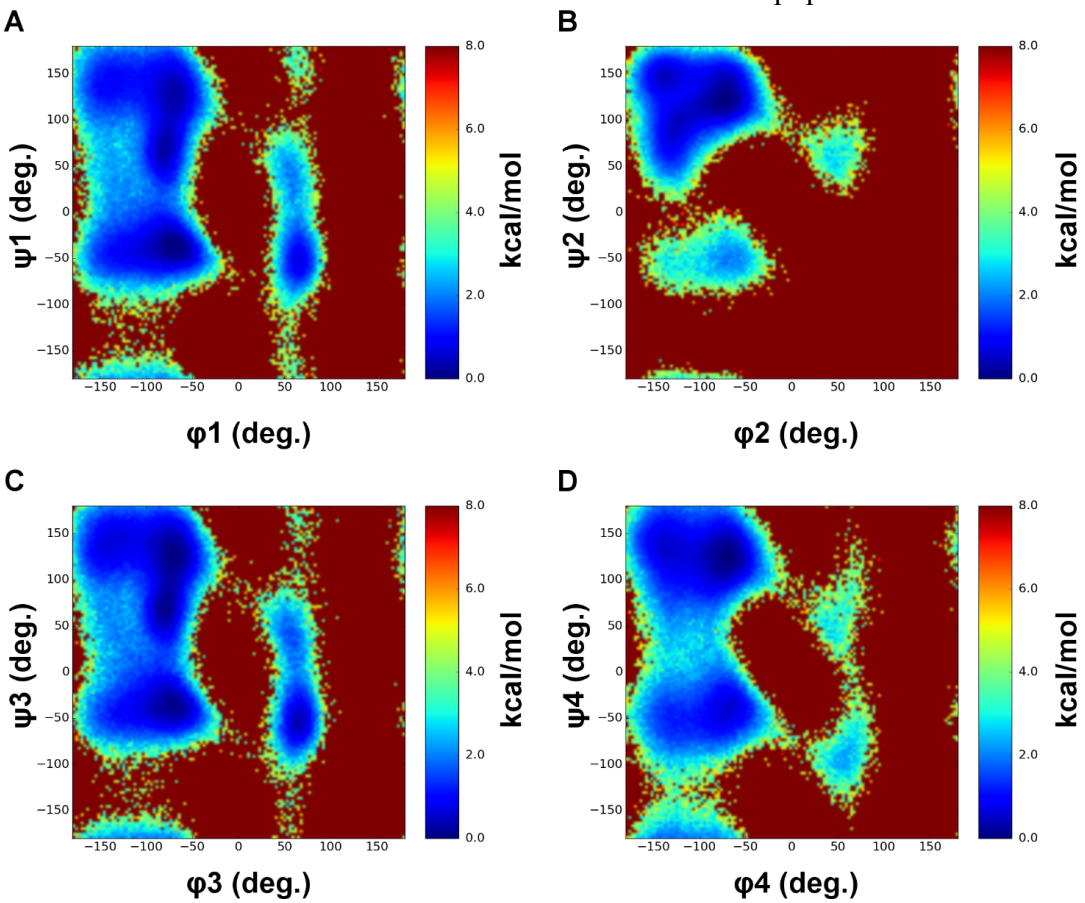

Figure S19. Free energy surfaces of the Boltzmann reweighted distributions of φ and ψ dihedrals obtained from the aMD simulation of hexapeptide *E*-**12**.

Table S7. Consistency between NOE signals of **12** and distances[a] measured in cluster1 and cluster2 representative geometries, obtained from the aMD simulation of *E*-**12** [b]

NOE (strength)	Cluster1 (pop. = 44.3%)	Cluster2 (pop. = 29.2%)
β-Morph$_1$H2-NH$_{Leu2}$ (m)	✓ (2.4 ± 0.7)	✓ (3.0 ± 0.5)
NH$_{Leu2}$-Hα$_{Leu2}$ (m)	✓ (2.9 ± 0.1)	✓ (3.0 ± 0.2)
NH$_{Leu2}$-NH$_{Val3}$ (w)	✓ (3.6 ± 0.7)	✓ (2.5 ± 0.4)
Hα$_{Leu2}$-NH$_{Val3}$ (m)	✓ (2.4 ± 0.2)	**?** (3.5 ± 0.2)
Hα$_{Val3}$-β-Morph$_4$H5 (m)	**?** (4.7 ± 2.5)	✓ (1.9 ± 0.2)
β-Morph$_4$H2-NH$_{Leu5}$ (w)	✓ (3.6 ± 0.5)	✓ (3.5 ± 0.5)
NH$_{Leu5}$-NH$_{Val6}$ (w)	✓ (3.7 ± 0.7)	**?** (4.5 ± 0.8)
NH$_{Leu5}$-Hα$_{Leu5}$ (m)	✓ (2.9 ± 0.1)	✓ (2.9 ± 0.1)
(CH$_2$)$_{Leu5}$-NH$_{Val6}$ (m)[c]	**?** (4.4 ± 0.9)	**?** (4.2 ± 0.7)
Hα$_{Leu5}$-NH$_{Val6}$ (m)	✓ (1.9 ± 0.8)	✓ (2.1 ± 0.6)

a. All distances, in Å are taken from the non-minimized most representative conformation of each cluster, while intervals are the mean deviations of the whole cluster population from the centroid. b. ✓ computed distance is compatible with NOE signal. ✗ computed distance is larger than expected for matching NOE signal. **?** computed distance is larger than expected, but might be compatible with NOE signal. NOE signals are classified as strong (s), medium (m) and weak (w). c Distances are averaged among both methylene hydrogens.

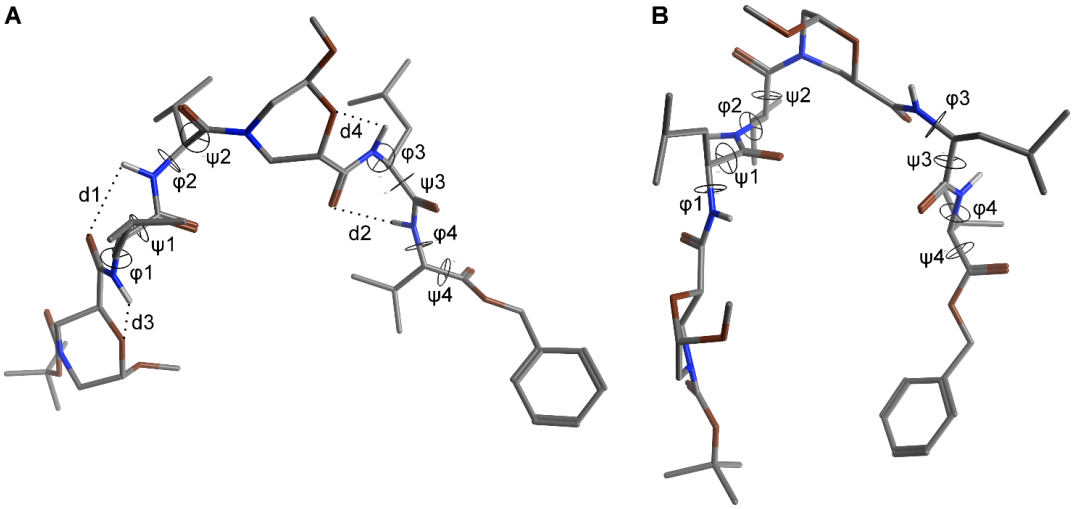

Figure S20. A) Representative conformations of cluster2 (pop. = 16.9%) obtained from the analysis of the 750-1000 ns segment of the aMD trajectory of hexapeptide *Z*-**12'**. Selected geometrical parameters are: d1 = 3.5 ± 0.8; d2 = 3.8 ± 0.8; d3 = 2.2 ± 0.5; d4 = 2.4 ± 0.3; φ1 = -72.3 ± 24.5; ψ1 = 128.5 ± 29.6; φ2 = -83.1 ± 22.7; ψ2 = 122.0 ± 17.5; φ3 = -69.2 ± 25.8; ψ3 = 139.2 ± 54.9; φ4 = -97.8 ± 26.6; ψ4 = 130.6 ± 61.5. Distances are reported in Å, dihedrals in deg. The values are taken from the non-minimized most representative conformation, while intervals are the mean deviations of the whole cluster population from the centroid. B) Representative conformation of cluster3 (pop. = 14.6%) for the same system; d1 = 3.5 ± 0.7; d2 = 3.0 ± 0.8; d3 = 2.9 ± 0.5; d4 = 2.4 ± 0.6; φ1 = -81.1 ± 24.5; ψ1 = 125.2 ± 22.6; φ2 = -88.0 ± 19.6; ψ2 = 117.6 ± 15.5; φ3 = -48.5 ± 35.5; ψ3 = 104.2 ± 64.7; φ4 = -73.5 ± 27.5; ψ4 = 142.8 ± 69.5.

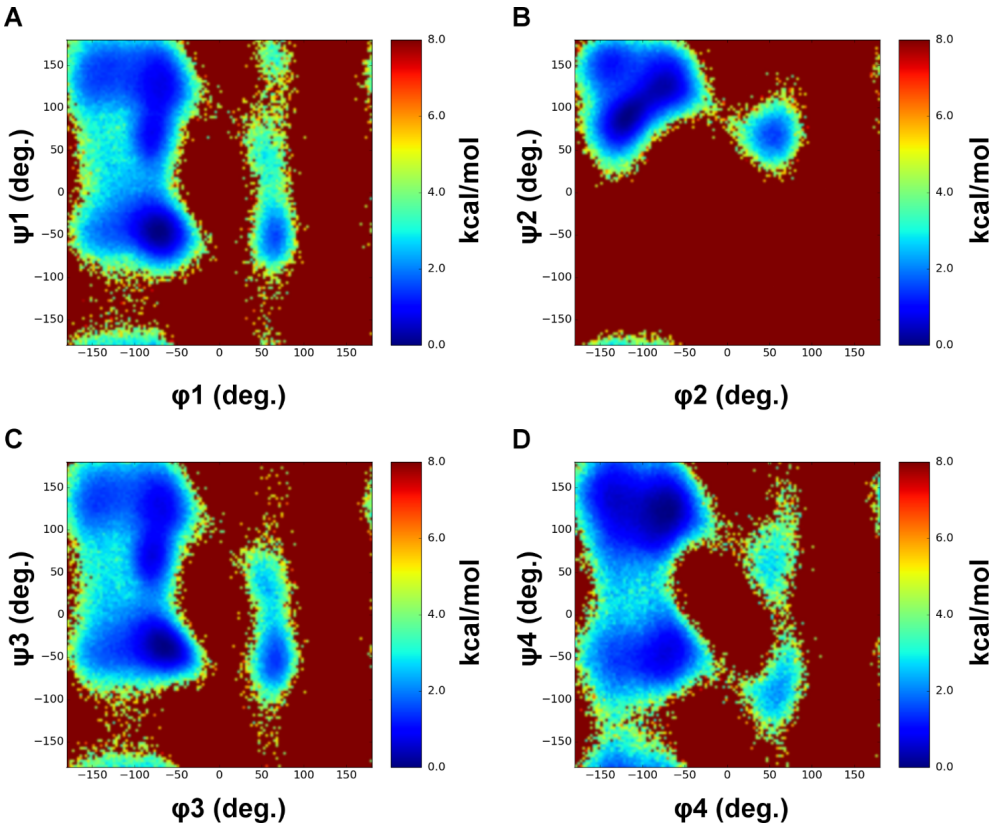

Figure S21. Free energy surfaces of the Boltzmann reweighted distributions of φ and ψ dihedrals obtained from the aMD simulation of *Z*-**12**.

Table S8. Consistency between NOE signals and distances[a] measured in cluster1 (pop. = 38.3%), cluster2 (pop. = 16.9%) and cluster3 (pop. = 14.6%), obtained from the aMD of *Z*-**12**.[b]

NOE (strength)	Cluster1	Cluster2	Cluster2
β-Morph$_1$H6-Leu$_2$NH (w)	**?** (4.6 ± 0.6)	✓ (3.7 ± 0.6)	**?** (4.7 ± 0.6)
β-Morph$_1$H2-Leu$_2$NH (m)	✓ (2.4 ± 0.5)	✓ (3.3 ± 0.5)	✓ (2.6 ± 0.5)
Leu$_2$NH-Leu$_2$Hα (m)	✓ (2.8 ± 0.1)	✓ (2.8 ± 0.1)	✓ (2.9 ± 0.1)
Leu$_2$NH-Val$_3$NH (w)	✓ (2.5 ± 0.6)	✓ (4.4 ± 0.3)	**?** (4.5 ± 0.2)
Leu$_2$Hα-Val$_3$NH (m)	✓ (3.4 ± 0.3)	✓ (2.2 ± 0.2)	✓ (2.2 ± 0.2)
Leu$_2$CH$_2$-Val$_3$NH (w)[c]	✓ (2.9 ± 1.0)	**?** (4.2 ± 0.5)	✓ (3.7 ± 0.8)
Val$_3$Hα-β-Morph$_4$H3 (s)	✓ (1.9 ± 0.2)	✓ (2.5 ± 0.5)	✓ (2.0 ± 0.2)
β-Morph$_4$H2-Leu$_5$NH (m)	✓ (2.1 ± 0.1)	✓ (3.4 ± 0.5)	✓ (2.8 ± 0.5)
β-Morph$_4$H6-Leu$_5$NH (vw)	✓ (5.2 ± 0.4)	✓ (3.9 ± 0.5)	✓ (4.1 ± 0.8)
Leu$_5$NH-Val$_6$NH (w)	✓ (3.1 ± 0.5)	**?** (4.7 ± 0.8)	**?** (4.5 ± 0.9)
Leu$_5$NH-Leu$_5$Hα (s)	✓ (2.8 ± 0.1)	✓ (2.8 ± 0.1)	✓ (2.5 ± 0.4)
Leu$_5$CH$_2$-Val$_6$NH (w)[c]	✓ (3.7 ± 0.6)	✓ (3.6 ± 0.8)	**?** (4.5 ± 0.5)
Leu$_5$Hα-Val$_6$NH (m)	**?** (3.7 ± 0.3)	✓ (2.4 ± 0.4)	✓ (2.3 ± 0.5)

a. All distances, in Å are taken from the non-minimized most representative conformation of each cluster, while intervals are the mean deviations of the whole cluster population from the centroid. b. ✓ computed distance is compatible with NOE signal. ✗ computed distance is larger than expected for matching NOE signal. **?** computed distance is larger than expected, but might be compatible with NOE signal. NOE signals are classified as strong (s), medium (m) and weak (w). c Distances are averaged among both methylene hydrogens.

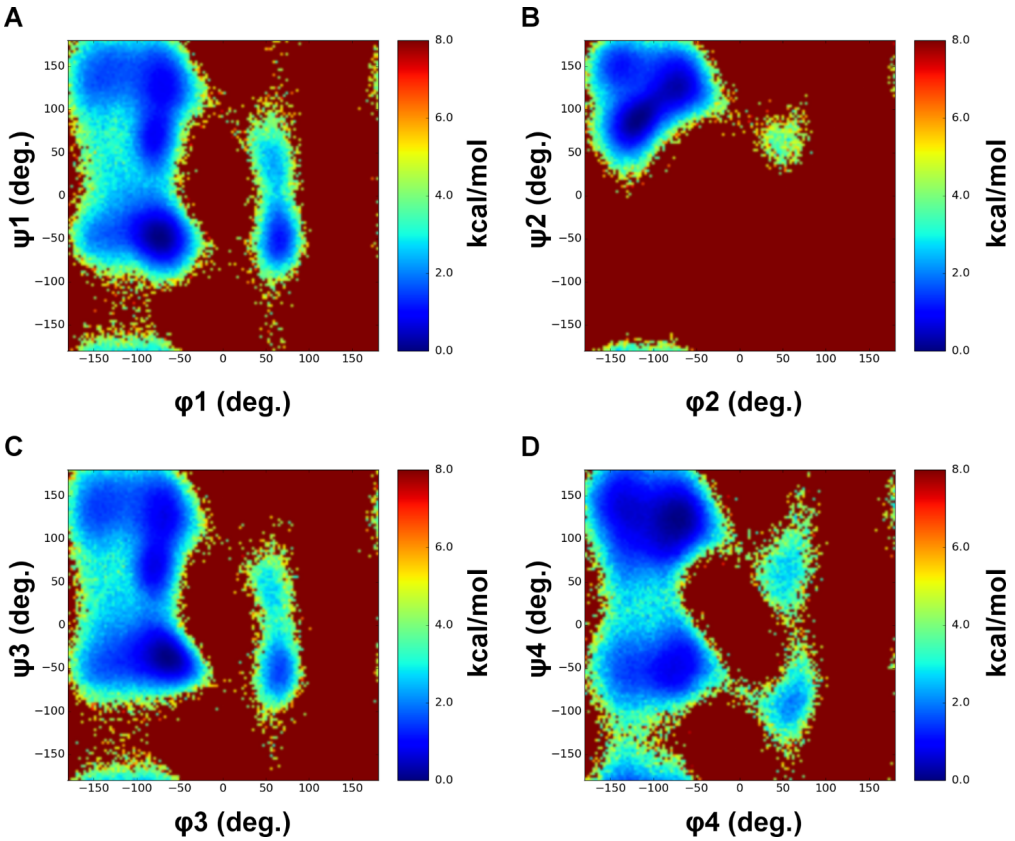

Figure S22. Free energy surfaces of the Boltzmann reweighted distributions of φ and ψ dihedrals obtained from the aMD simulation of *Z*1,*Z*4-**12'**, having a *Z* configuration at both BOC-β-Morph1 and Val3- β-Morph4 ω dihedrals.

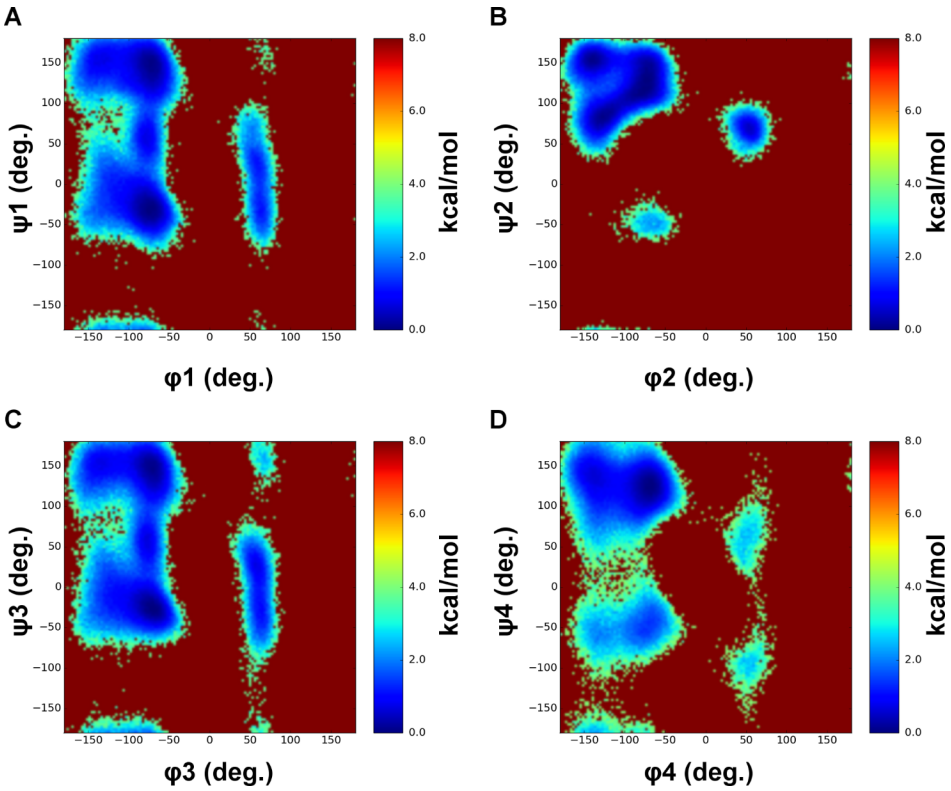

Figure S23. Free energy surfaces of the distributions of φ and ψ dihedrals obtained from the analysis of the 1.5-2.0 μs sector of the H-REMD trajectory of hexapeptide **12**. In this portion, simulations started from *trans* or *cis* configurations of ω1 and ω4 dihedrals were fully converged. H-REMD simulations were conducted in explicit CH_3CN, by running 12 replicas where the torsional energy function of all the φ, ψ and ω dihedrals was multiplied by $0.1 \leq \lambda \leq 1$ (λ=0.1 and λ=1 in replicas 1 and 12, respectively). The analyses were conducted on the unbiased replica (replica 12).

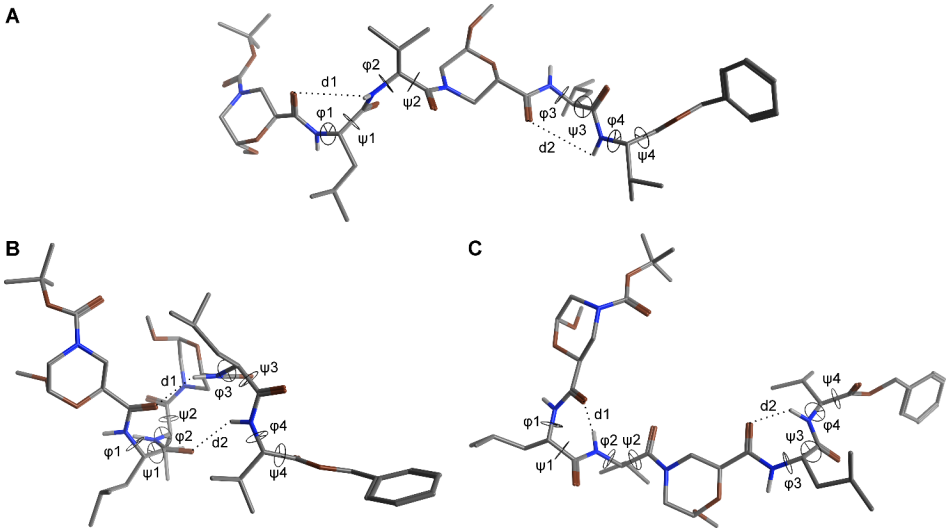

Figure S24. A) Representative conformations of cluster1 (pop. = 22.8%) obtained from the analysis of the 1500-2000 ns segment of the H-REMD trajectory of hexapeptide **12**. Selected geometrical parameters are: d1 = 3.8 ± 0.6; d2 = 3.4 ± 0.7; φ1 = -73.9 ± 24.1; ψ1 = 135.6 ± 23.6; φ2 = -76.1 ± 23.7; ψ2 = 122.9 ± 18.4; φ3 = -73.0 ± 29.3; ψ3 = 133.6 ± 69.9; φ4 = -63.9 ± 34.3; ψ4 = 141.5 ± 37.4. Distances are reported in Å, dihedrals in deg. The values are taken from the non-minimized most representative conformation, while intervals are the mean deviations of the whole cluster population from the centroid. B) Representative conformation of cluster2 (pop. = 20.2%); d1 = 2.2 ± 0.5; d2 = 3.3 ± 2.4; φ1 = -81.4 ± 12.8; ψ1 = -54.5 ± 63.8; φ2 = -119.5 ± 56.3; ψ2 = 96.0 ± 17.2; φ3 = -20.1 ± 65.0; ψ3 = -81.6 ± 83.7; φ4 = -75.9 ± 29.5; ψ4 = 129.5 ± 31.0. C) Representative conformation of cluster3 (pop. = 15.7%); d1 = 3.3 ± 0.6; d2 = 2.1 ± 1.6; φ1 = -62.0 ± 29.9; ψ1 = 32.3 ± 24.8; φ2 = -101.7 ± 30.7; ψ2 = 121.4 ± 27.6; φ3 = -71.3 ± 28.2; ψ3 = 74.7 ± 72.1; φ4 = -65.4 ± 32.5; ψ4 = 143.2 ± 35.6.

Computational methods

Parameterization of β-Morph. Charge parameterization for β-Morph was performed using the R.E.D.IV tools.[4] The amino acid structure was capped by acetyl and a NHMe group at the N and C termini, respectively, and subjected to a conformational search using the low mode method, the AMBER10EHT force field and the Born solvation model implemented in MOE.[5] The two conformations corresponding to the *E* and *Z* configurations at the peptide bond linking the acetyl cap to the residue were used for charge parameterization. For each conformation, two orientations were used to derive conformation and orientation independent RESP charges. Gaussian09[6] was used to perform quantum mechanical calculations at the HF/6-31G* level, accordingly to the force field specifications. All the molecular dynamics simulations were conducted with the Amber16 and AmberTools17 packages,[7] using the ff14SB forcefield.[8] Parameters for the peptide bond rotation were modified as suggested by Doshi and Hemelberg,[9]

Accelerated molecular dynamics. Peptide **7a** was prepared using *tleap* and solvated in an octahedral box of CH_3CN,[10] extending up to 10 Å. The system was equilibrated accordingly to a multistep protocol reported in detail elsewere.[11] A conventional MD run was then conducted for 20 ns, using the isothermal isobaric ensemble (NPT) to derive the boost parameters for the subsequent aMD run (average EPTOT = -11579.2 kcal/mol, average DHIED = 47.5 kcal/mol, total number of atoms = 2329, ethreshd = 65.0 kcal/mol, alphad = 3.5 kcal/mol, ethreshp = -11206.6 kcal/mol, alphap=372.6 kcal/mol). Production aMD simulations were conducted for 1 μs, under the NPT condition at 300 K, using a Langevin thermostat with a collision frequency of 2.0 ps-1, An electrostatic cutoff of 8.0 Å, the Particle mesh Ewald (PME) for long-range electrostatics,[12] and the SHAKE algorithm to constrain bonds involving hydrogens.[13] Simulations on *E*-**12,** *Z*-**12'** and *Z*1,*Z*4-**12'** were conducted under the same conditions, except for the different boost parameters (*E*-**12***:* average EPTOT = -16465.2 kcal/mol, average DHIED = 84.5 kcal/mol, total number of atoms = 3361, ethreshd=112.5 kcal/mol, alphad=5.6 kcal/mol, ethreshp = -15927.4 kcal/mol, alphap = 537.8 kcal/mol; *Z*-**12'**: average EPTOT = -16862.4 kcal/mol, average DHIED = 84.4 kcal/mol, total number of atoms = 3439, ethreshd=112.4 kcal/mol, alphad = 5.6 kcal/mol, ethreshp = -16312.2 kcal/mol, alphap = 550.2 kcal/mol; *Z*1,*Z*4-**12'**:

average EPTOT = -16558.3 kcal/mol, average DHIED = 84.6 kcal/mol, total number of atoms = 3379, ethreshd=112.6 kcal/mol, alphad = 5.6 kcal/mol, ethreshp = -16017.7 kcal/mol, alphap = 540.6 kcal/mol). The simulations were conducted using *pmemd.cuda* and analyzed with *cpptraj*.[7] Trajectories were clustered into 10 clusters using the average-linkage algorithm and the pairwise mass-weighted root mean squared deviation (RMSD) on the Cα. Convergence was evaluated by performing a cluster analysis every 250 ns and comparing results in terms of cluster population and RMSD between the main cluster representative conformations. All the simulations resulted converged within the chosen simulation time.

Hamiltonian replica exchange molecular dynamics. H-REMD simulations were conducted starting from the last frame of the 20 ns conventional MD described above for *E*-**12** and *Z*1,*Z*4-**12'**. The Hamiltonian was modified by progressively lowering the torsional potential of the φ, ψ and ω dihedrals over 12 replicas. Each replica was subjected to a geometry minimization (1000 cycles of steepest descent and 1000 cycles of conjugated gradient, up to a gradient of 0.1 kcal/mol·Å), followed by a 5 ns constant volume (NVT) equilibration (300 K, Langevin thermostat with a collision frequency = 2.0 ps^{-1}, electrostatic cutoff = 8.0 Å, PME, SHAKE to constrain bonds involving hydrogens). A production run of 2 μs was then conducted in the same conditions. Simulations were conducted on a HPC infrastructure using the *pmemd.MPI* software of the Amber16 package. Trajectory analyses were conducted on the final 500 ns of the unmodified replica, using *cpptraj* as described above for aMD simulations.

7. CD Spectra of peptide 12.

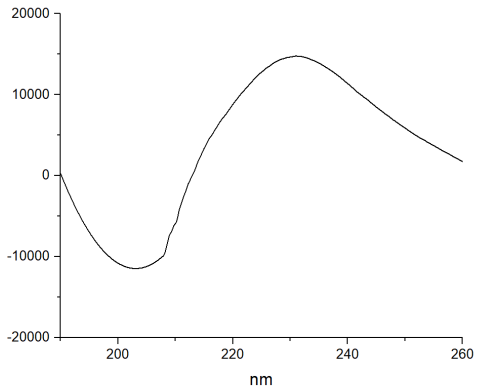

Figure S25 CD spectra of peptide **12** (100 μM in CH_3CN)

8. IR Spectrum of peptide 7a.

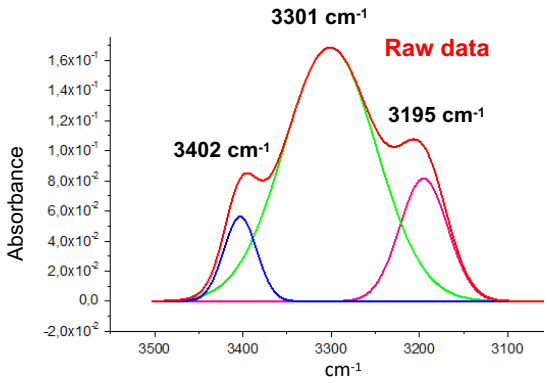

Figure S26. FTIR spectra of amide A portion acquired for peptide **7a**.

9. ^{1}H and ^{13}C NMR spectra

Compound (+)-4
1H in CDCl3 a T=300K

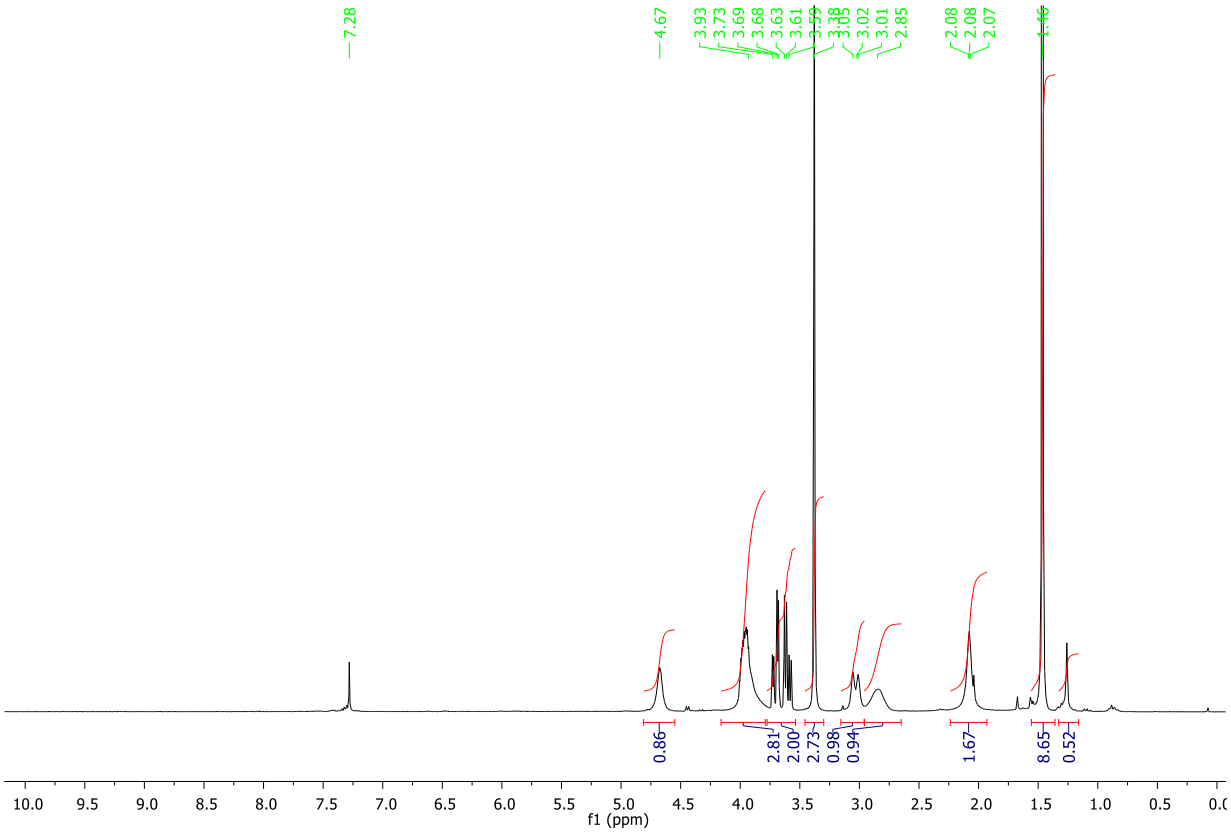

Compound (+)-4
13C-apt in CDCl3 a T=300K

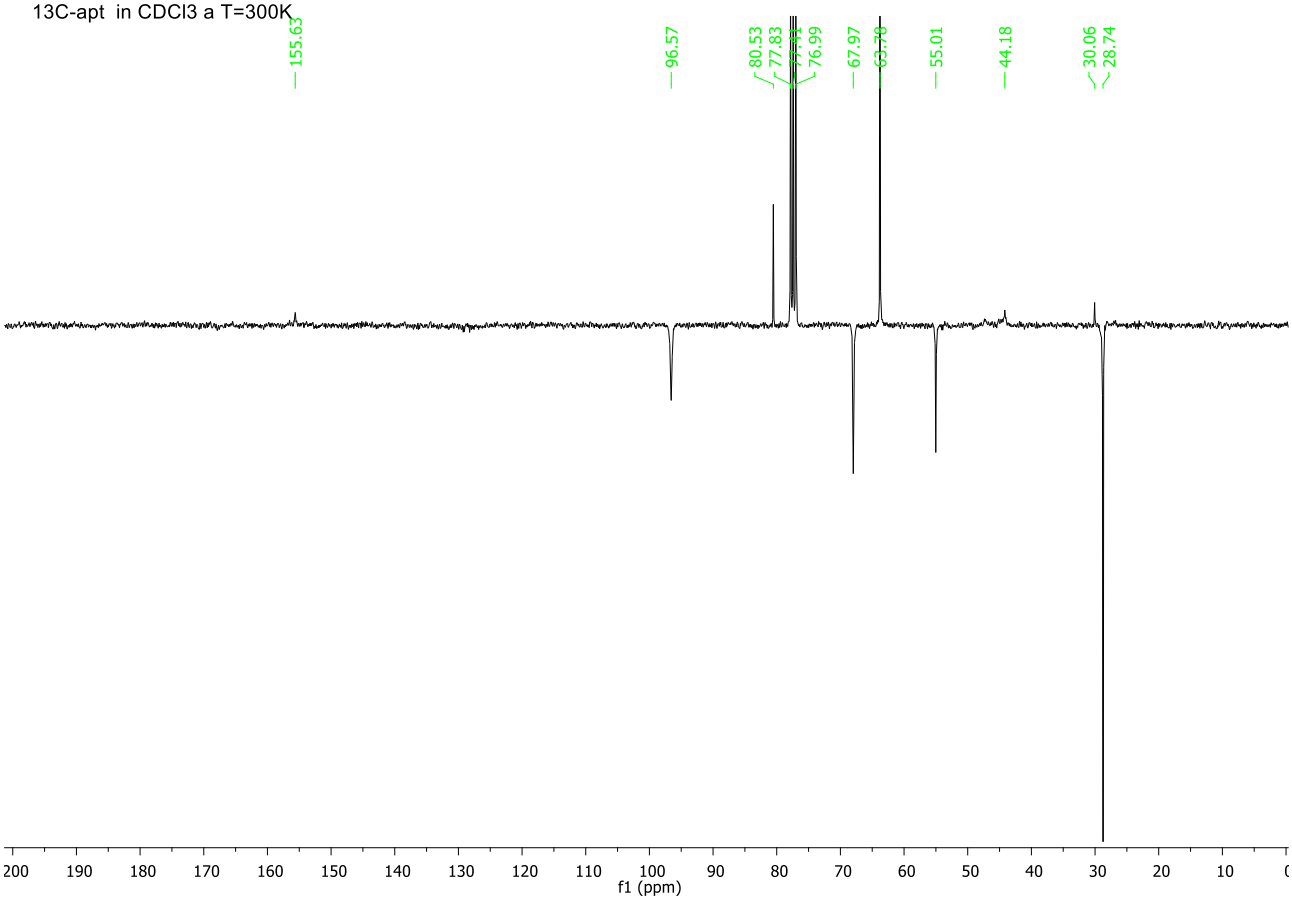

Compound (+)-5
1H in CDCl3 a T=300K

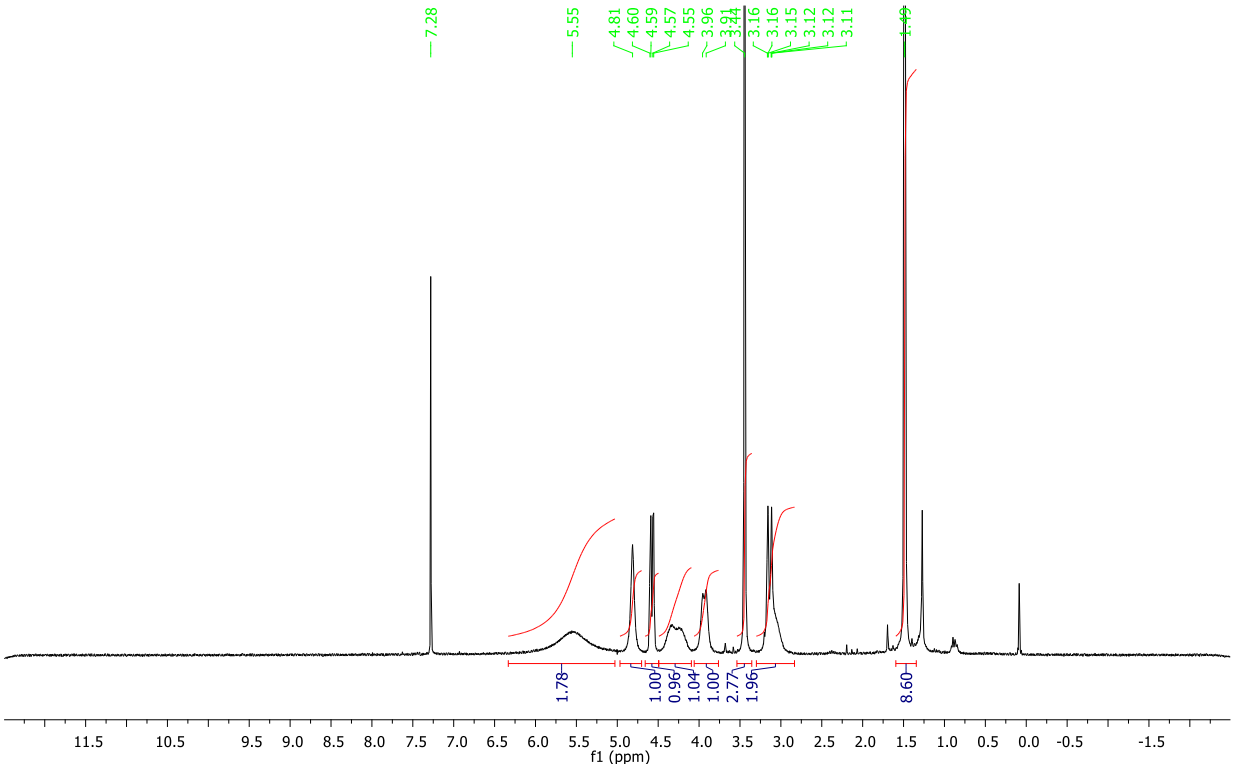

Compound (+)-5
13C-APT in CDCl3 a T=300K

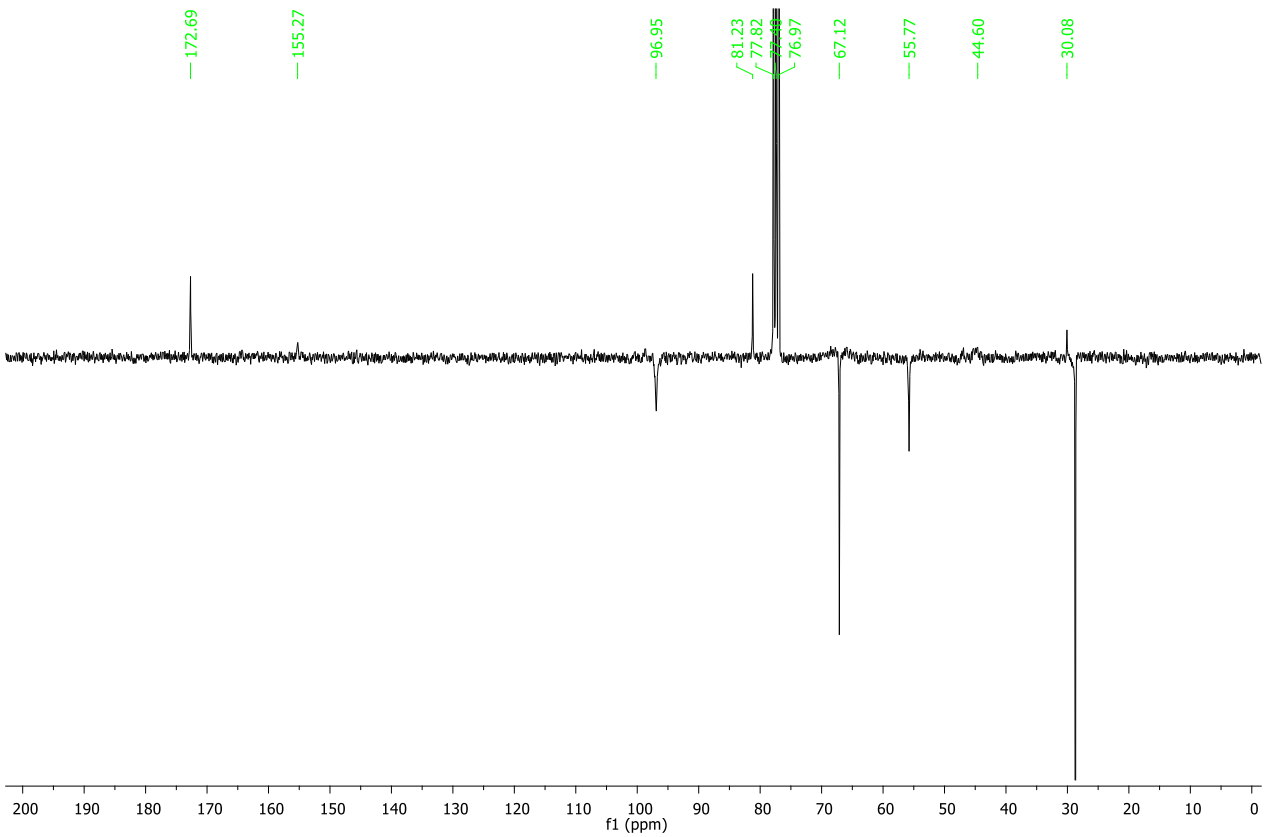

Compound 7a
1H in CD3CN a T=300K

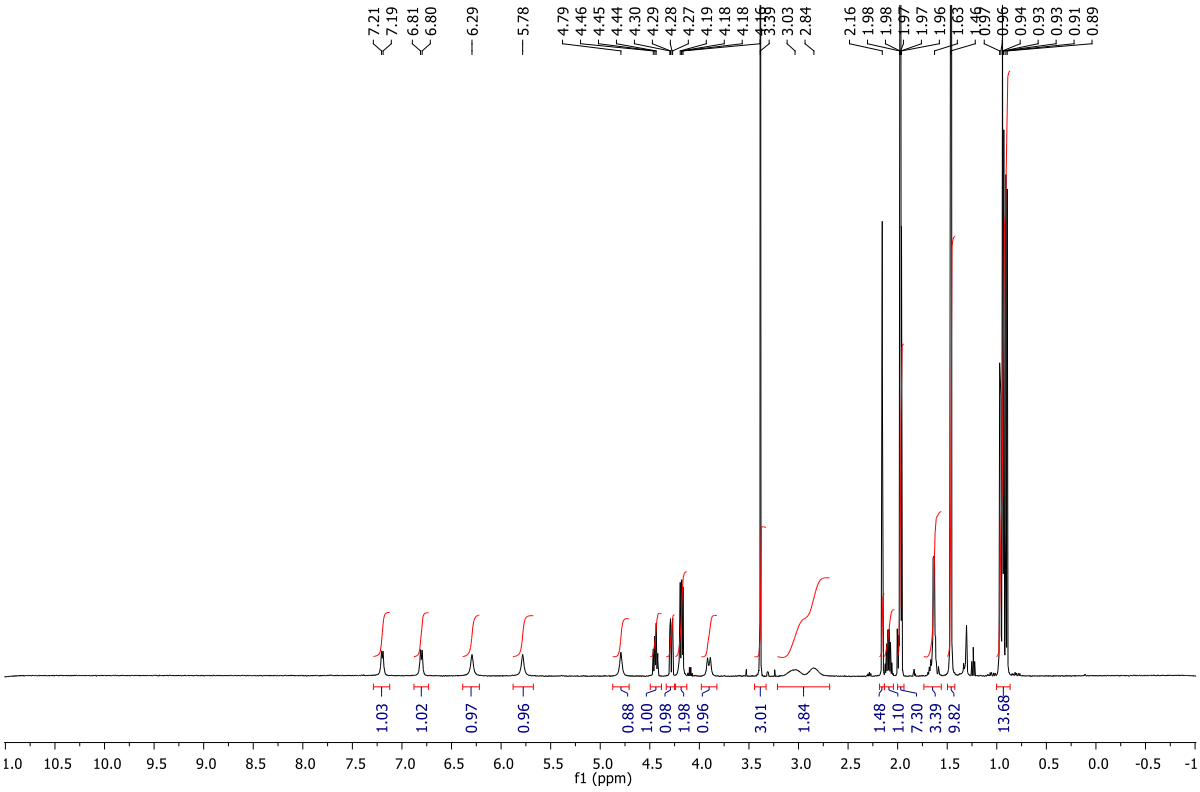

Compound 7a
13C-APT in CD3CN a T=300K

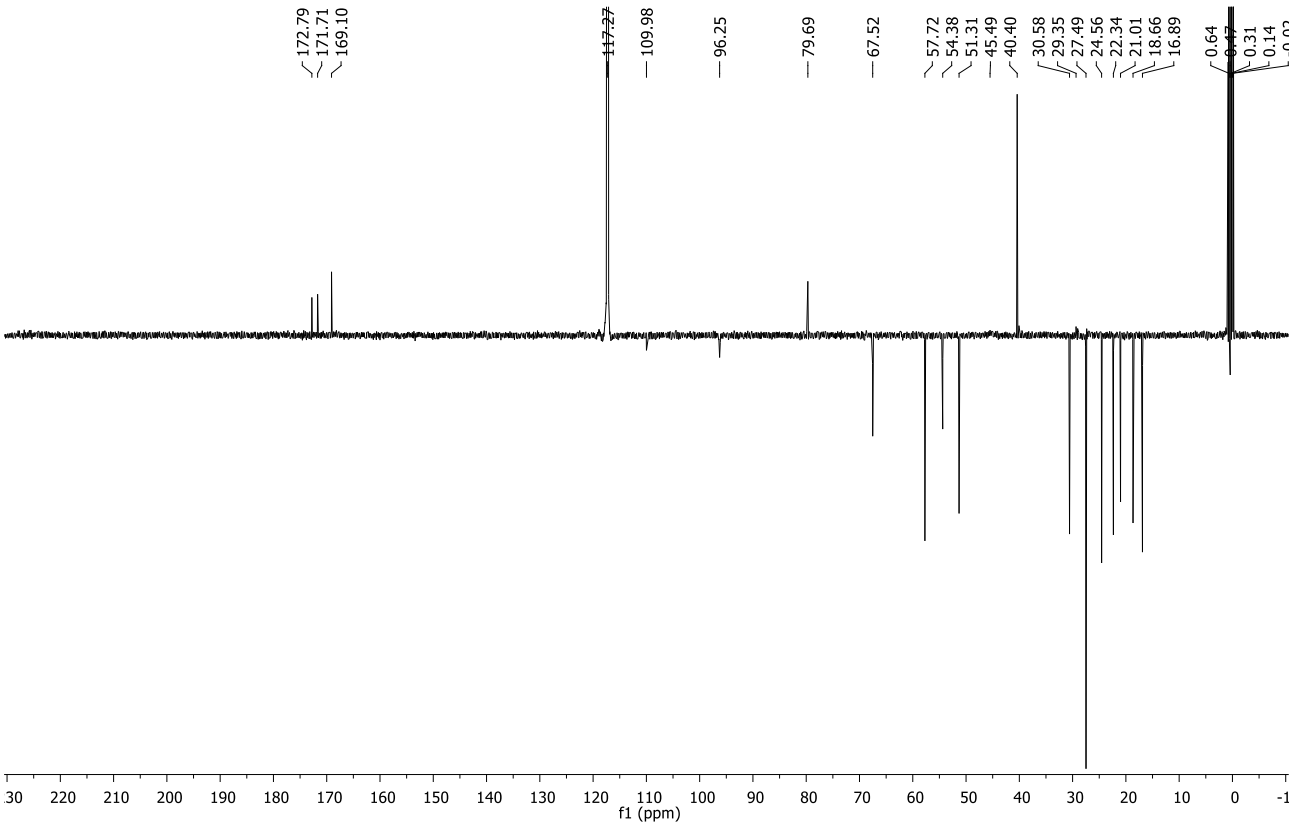

Compound 7b
1H in CD3CN a T=300K

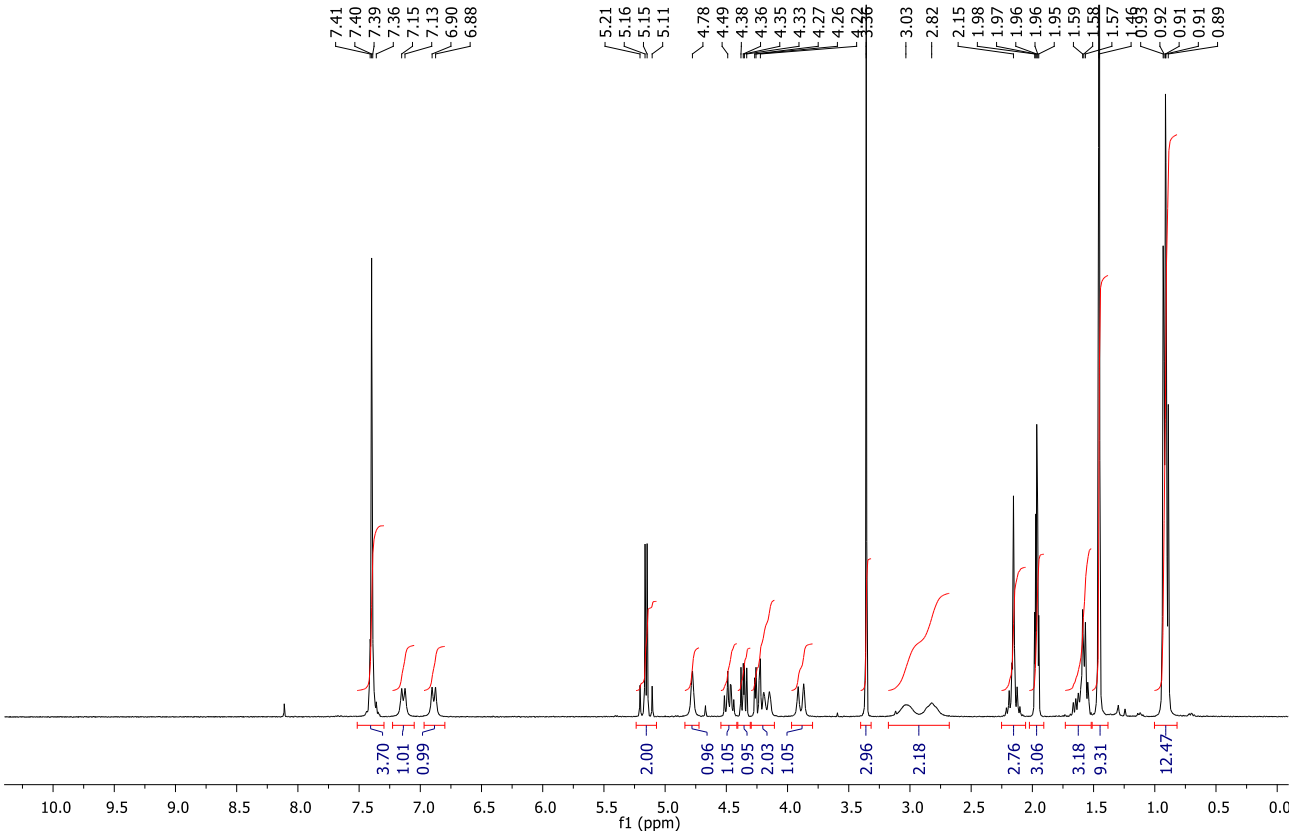

Compound 7b
13C-apt in CD3CN a T=300K

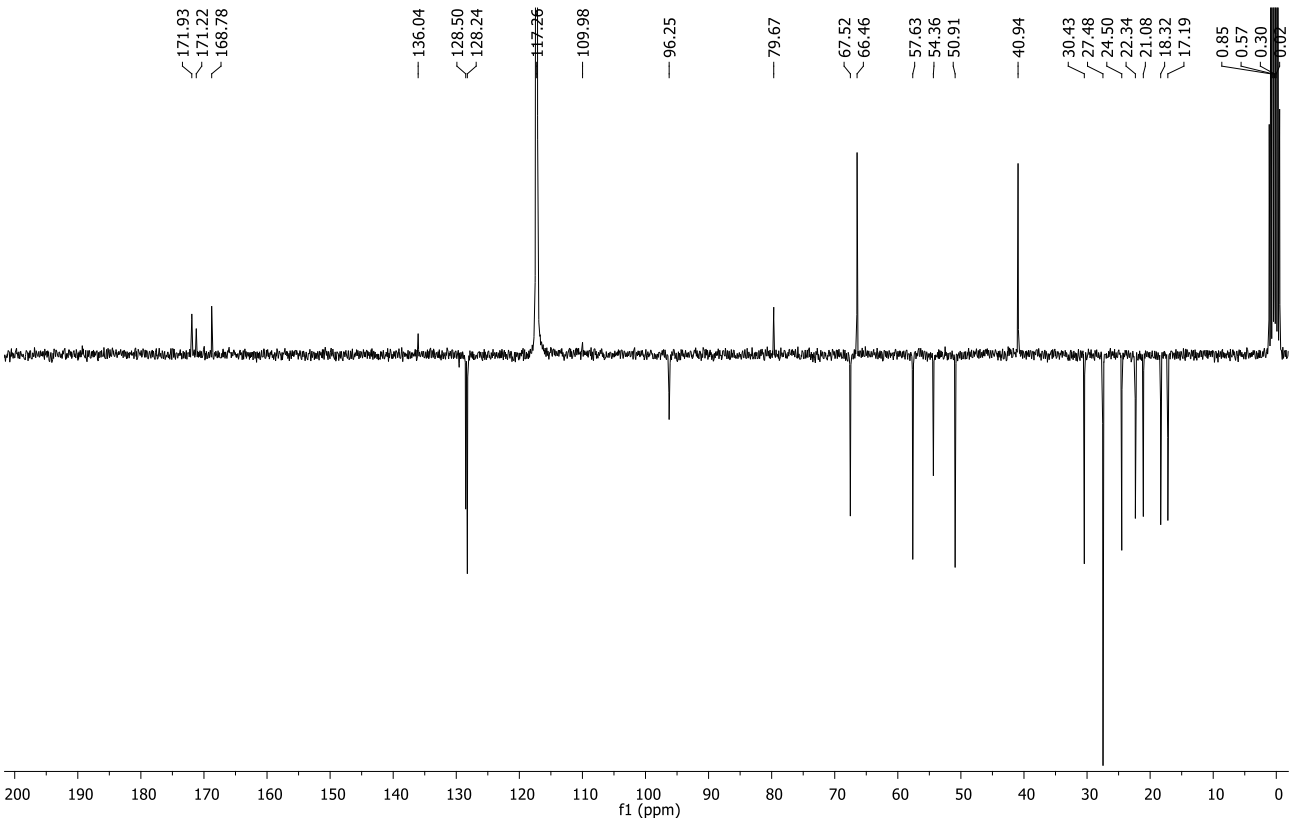

Compound 8a
1H in CD_3OD T=300K

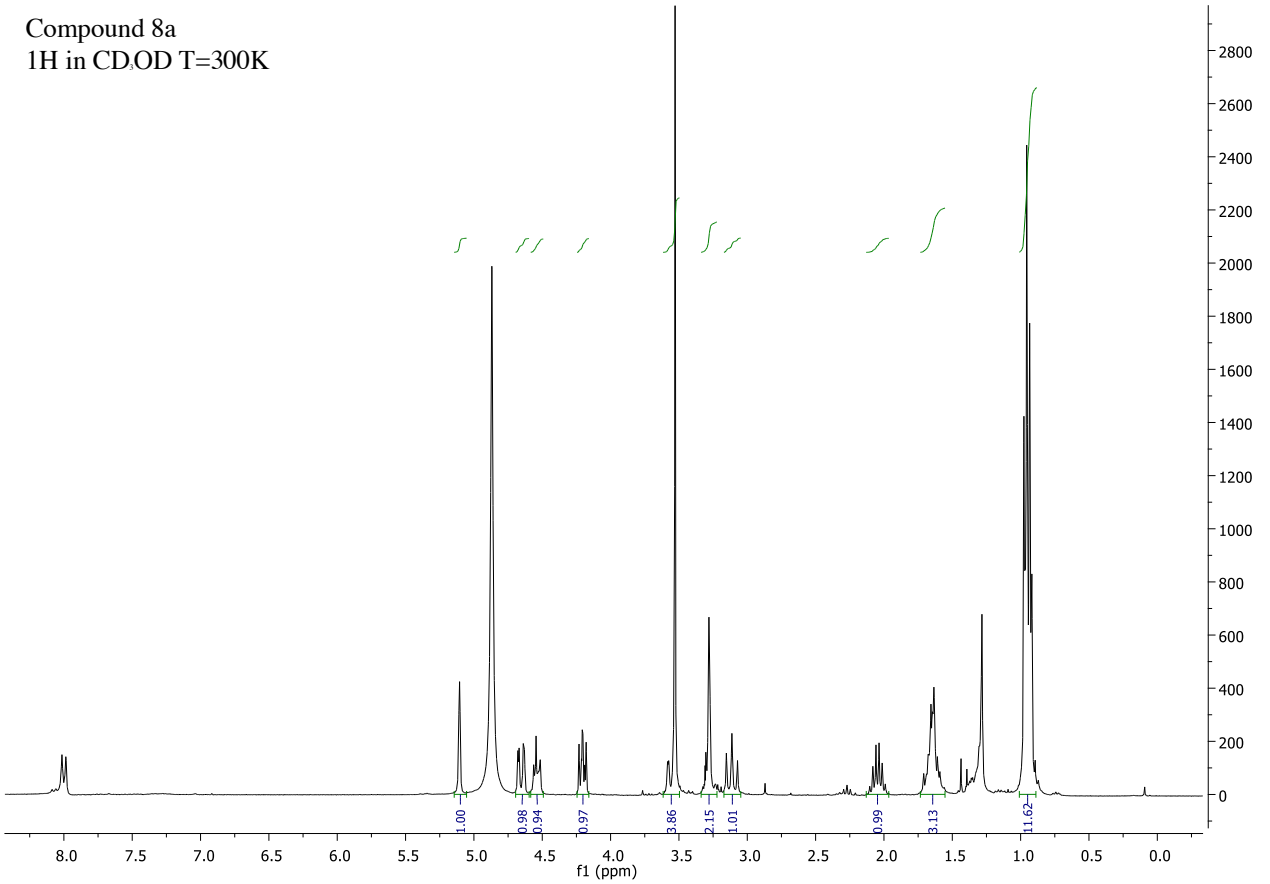

Compound 8a
13C in CD_3OD T=300K

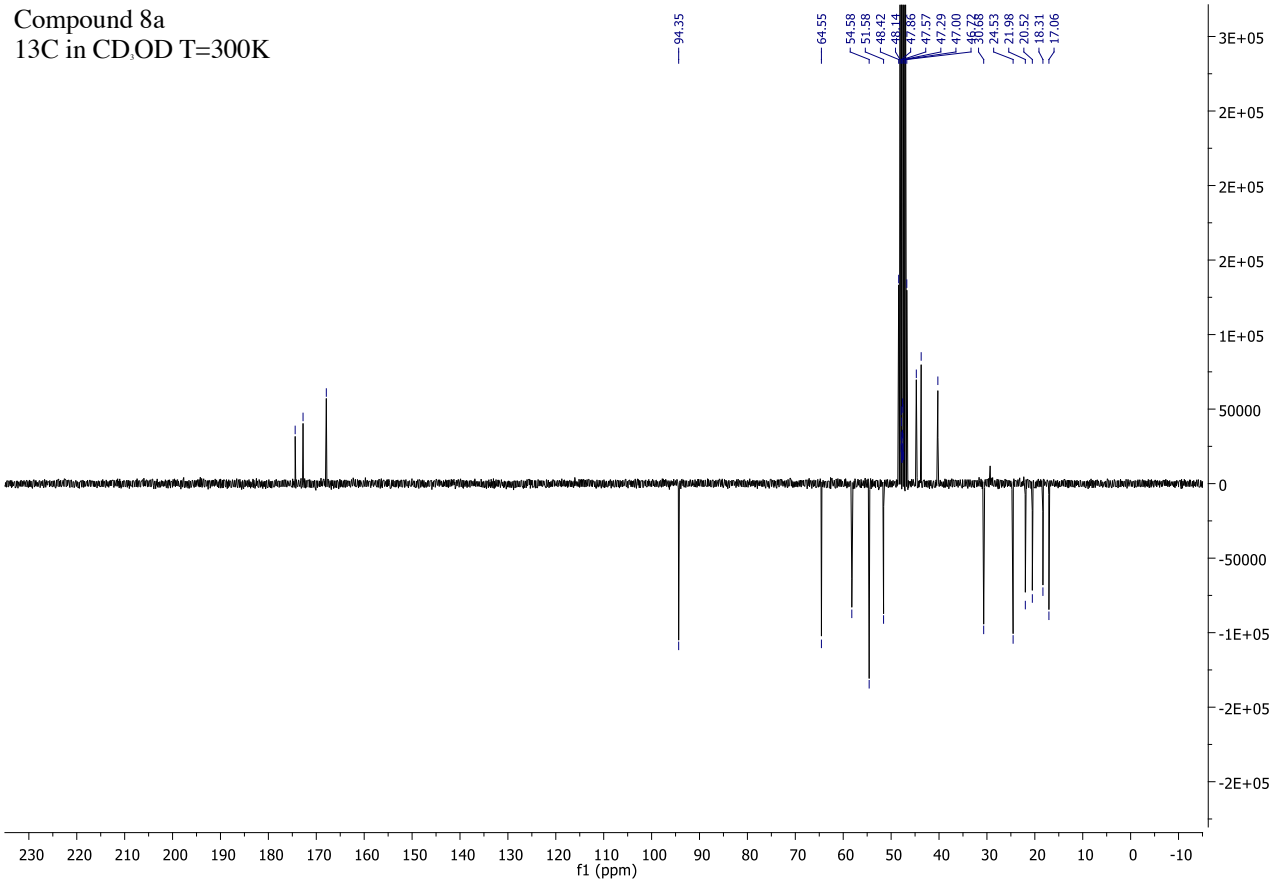

Compound 8b
1H in $CDCl_3$ T=300K

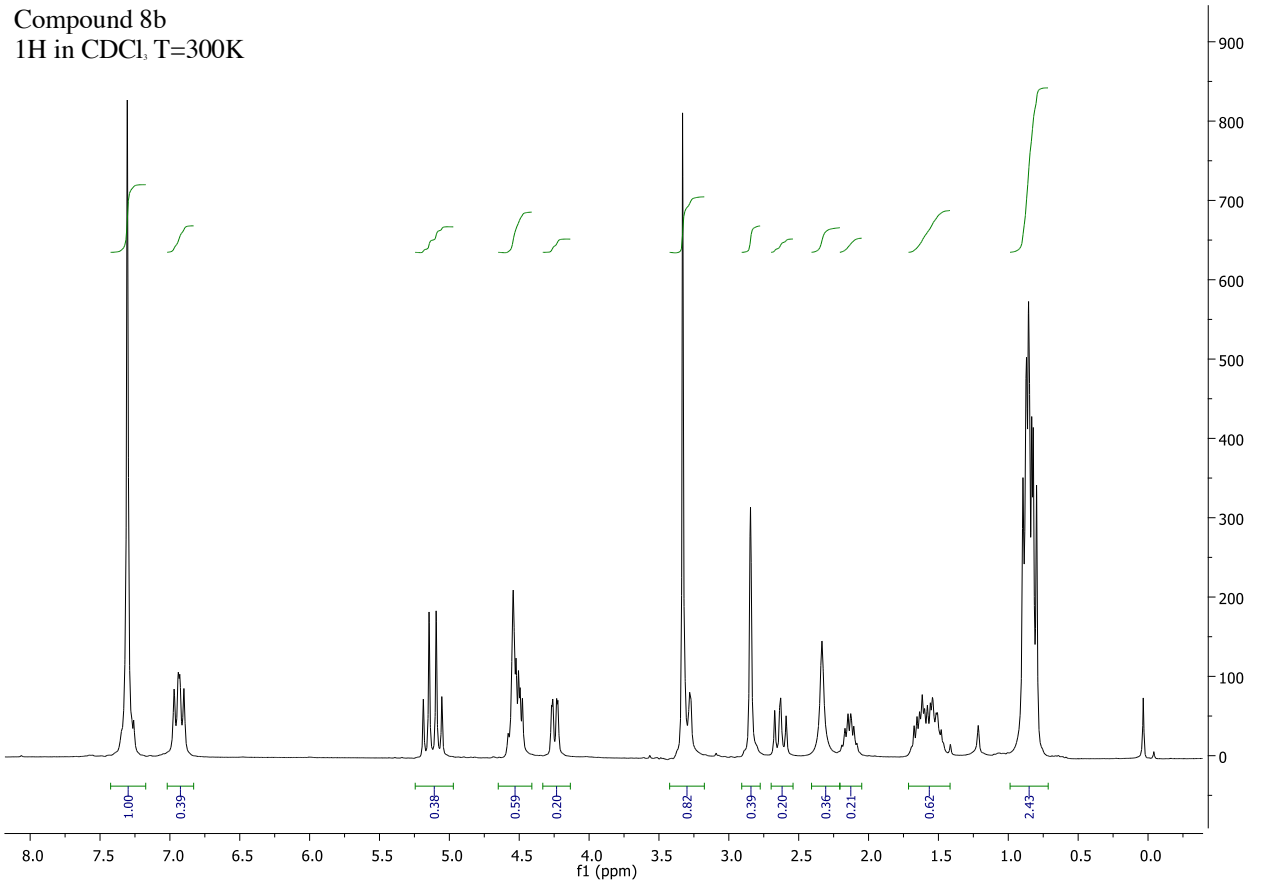

Compound 8b
13C in $CDCl_3$ T=300K

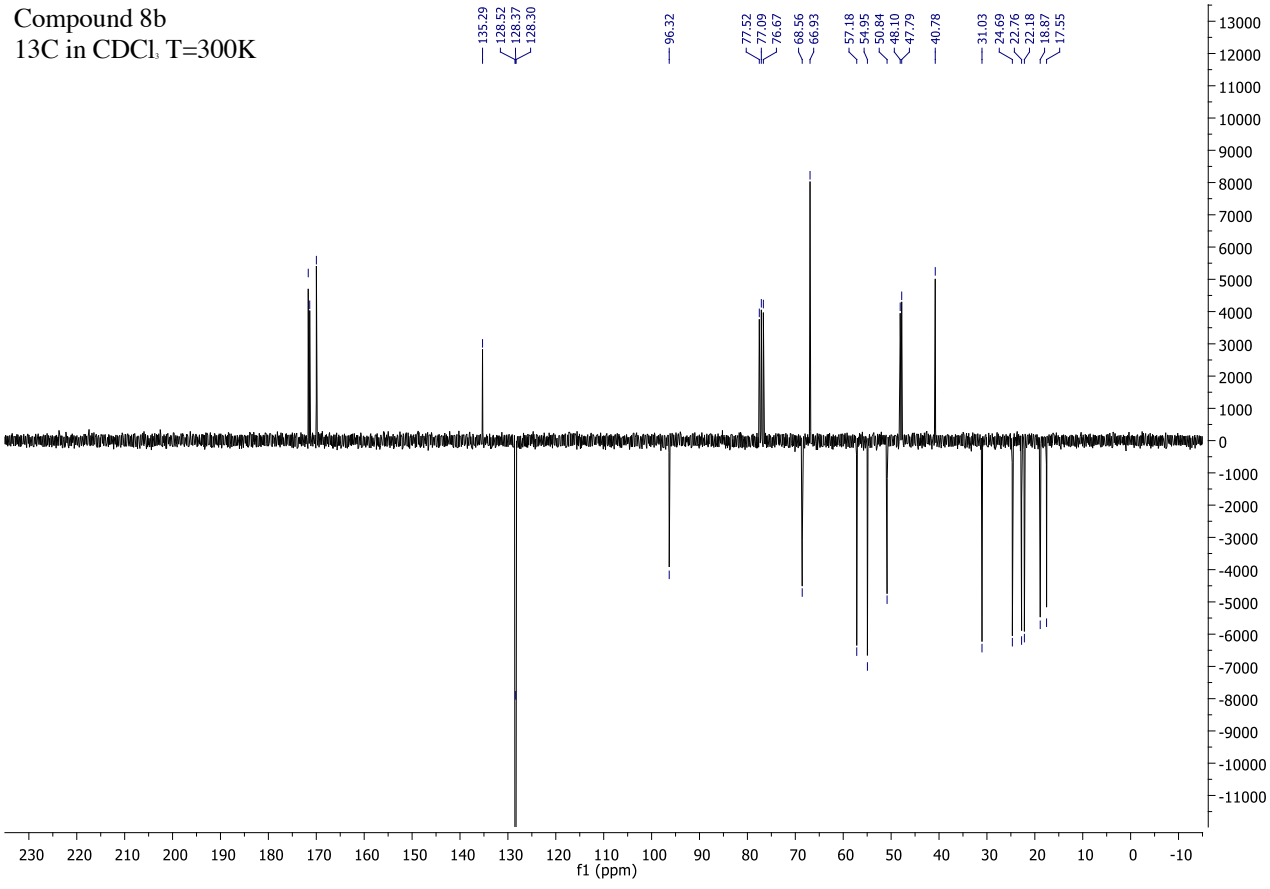

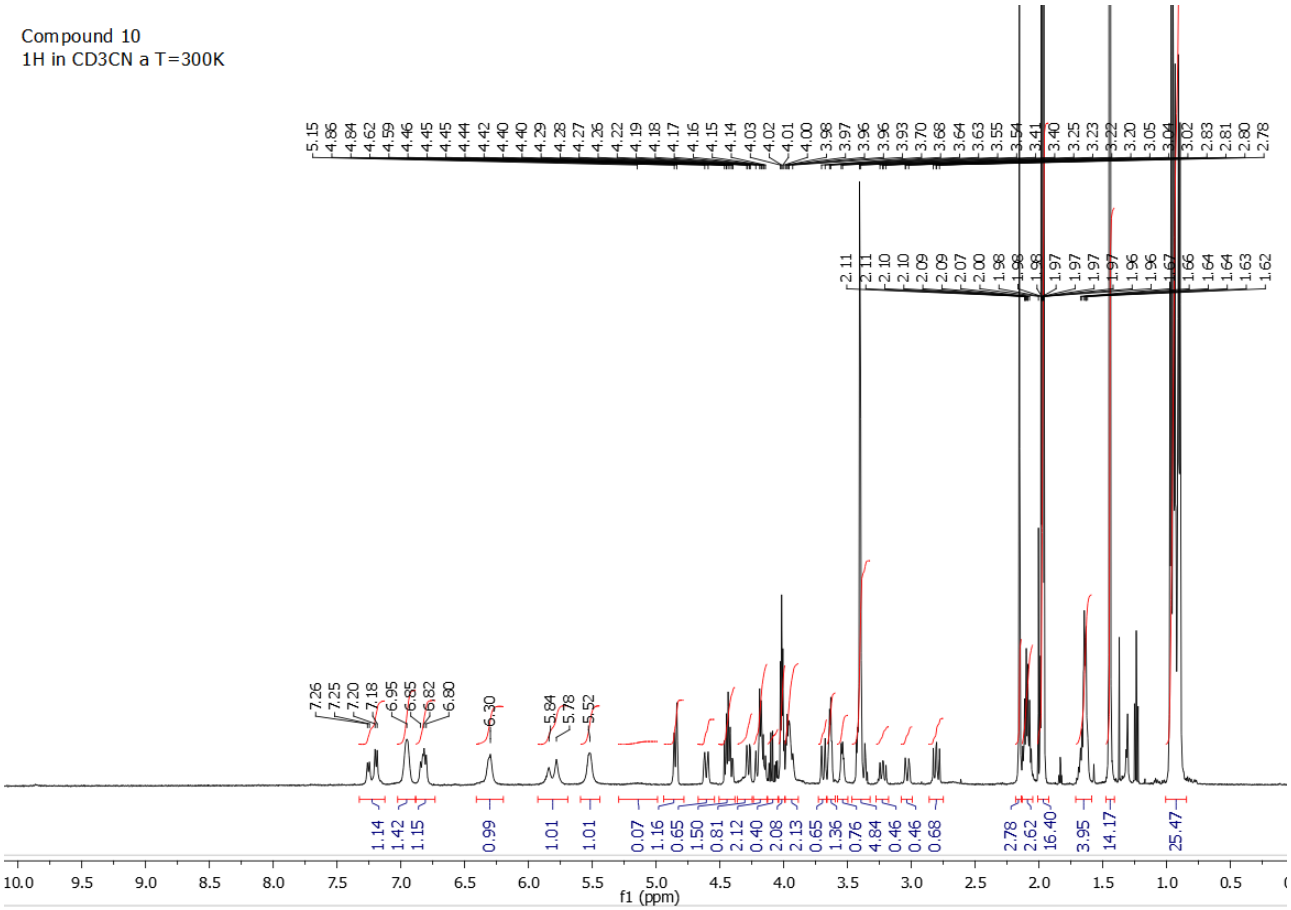
Compound 10
1H in CD3CN a T=300K
f1 (ppm)

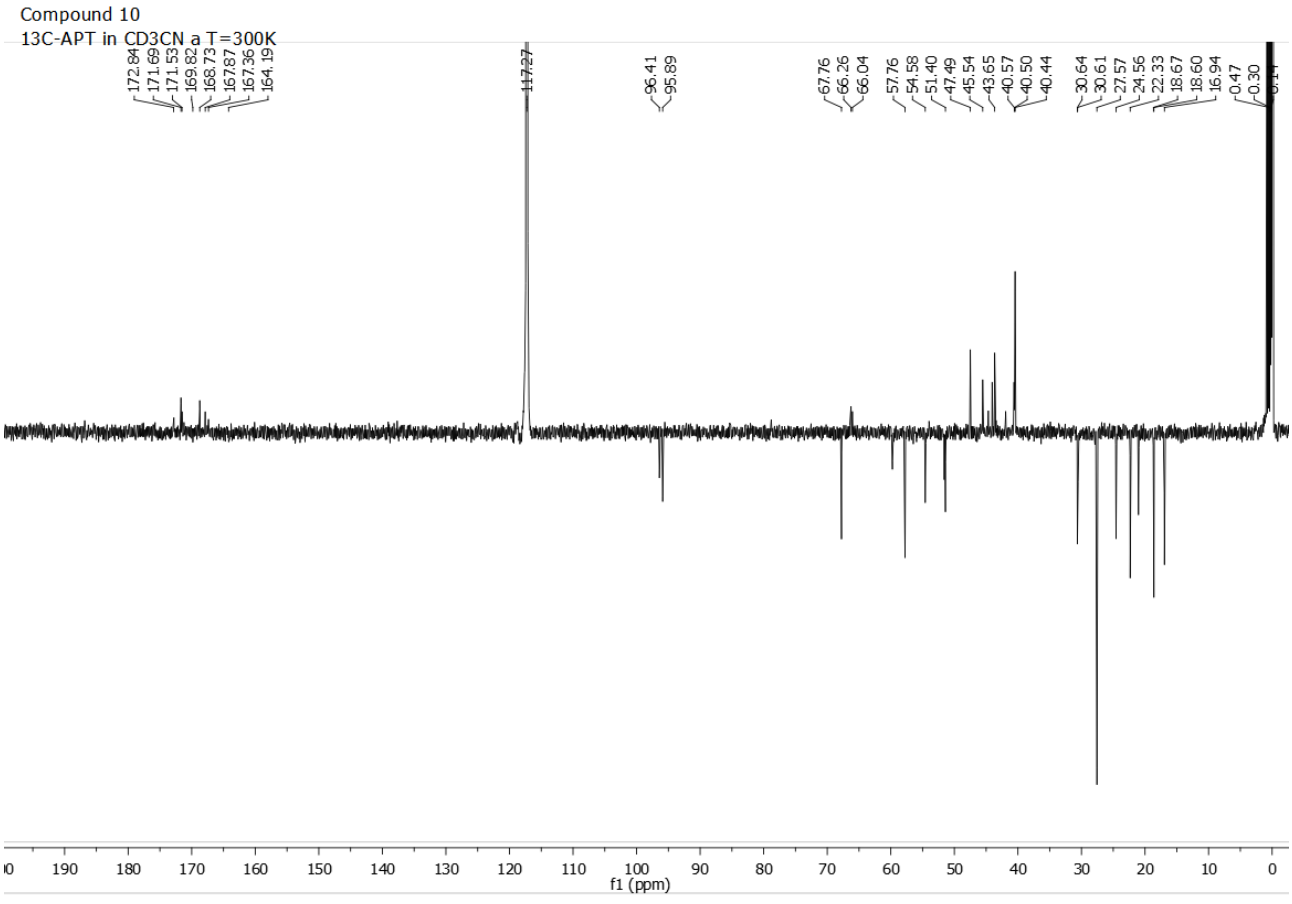
Compound 10
13C-APT in CD3CN a T=300K
f1 (ppm)

Compound 11
1H in $CDCl_3$ T=300K

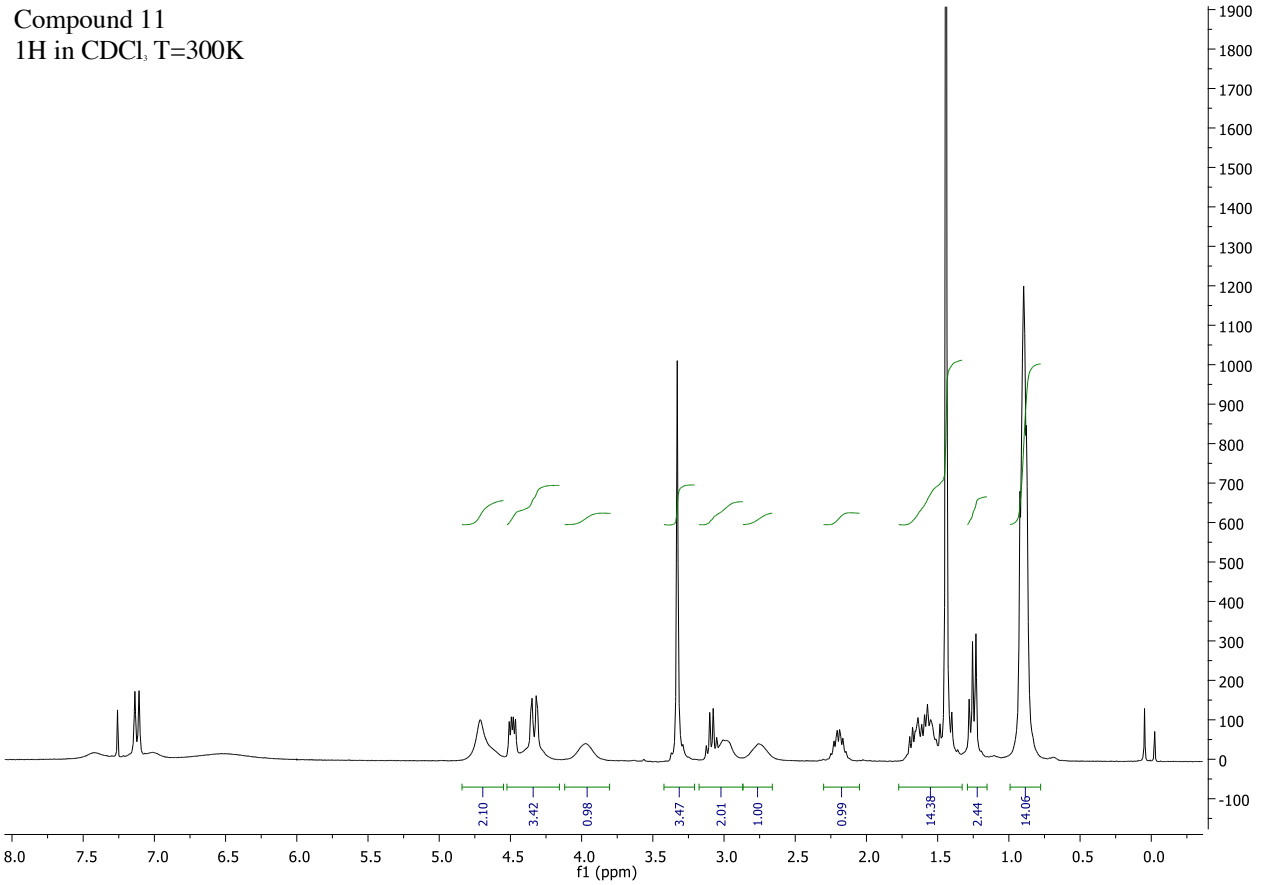

Compound 11
13C in CDCl3 T=300K

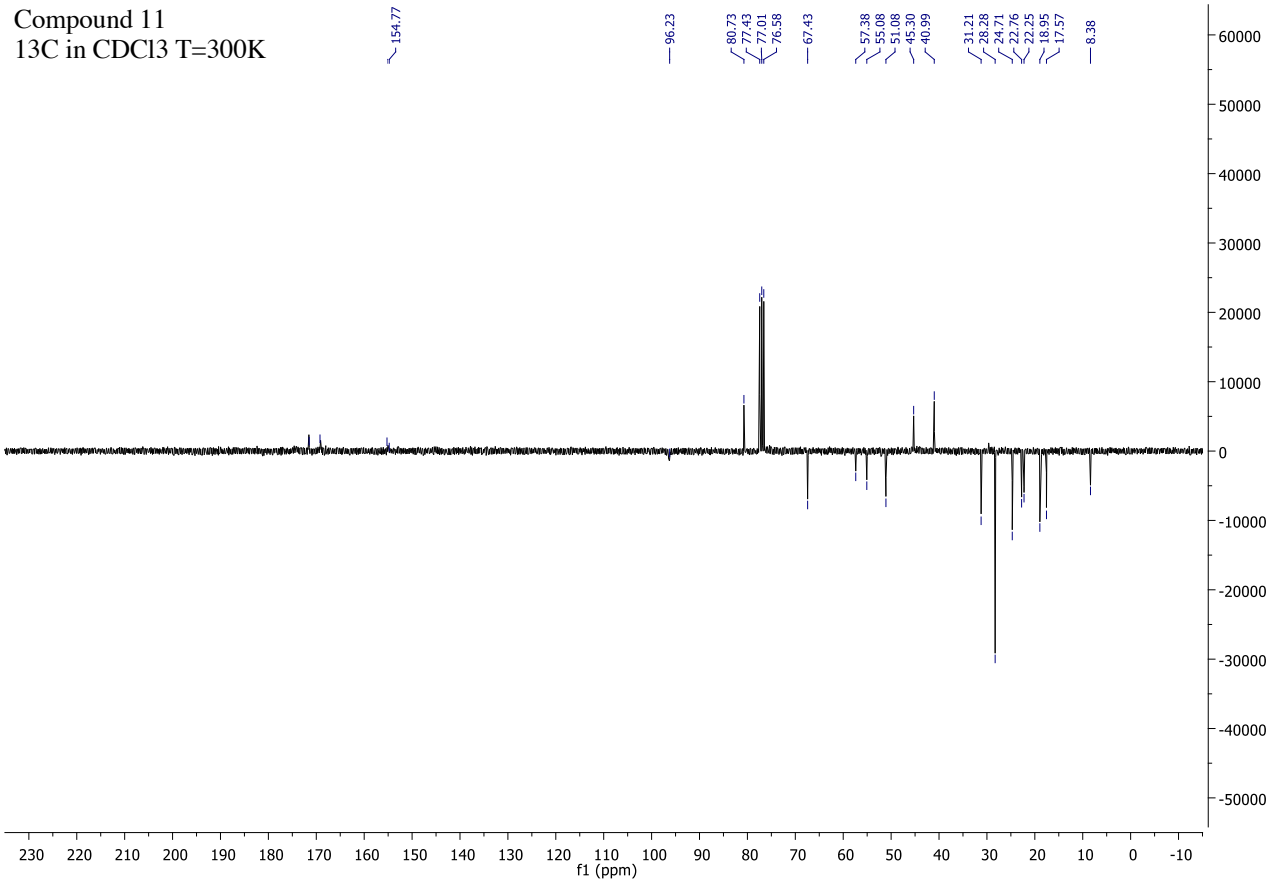

Compound 12
1H in CD_3CN T=300K

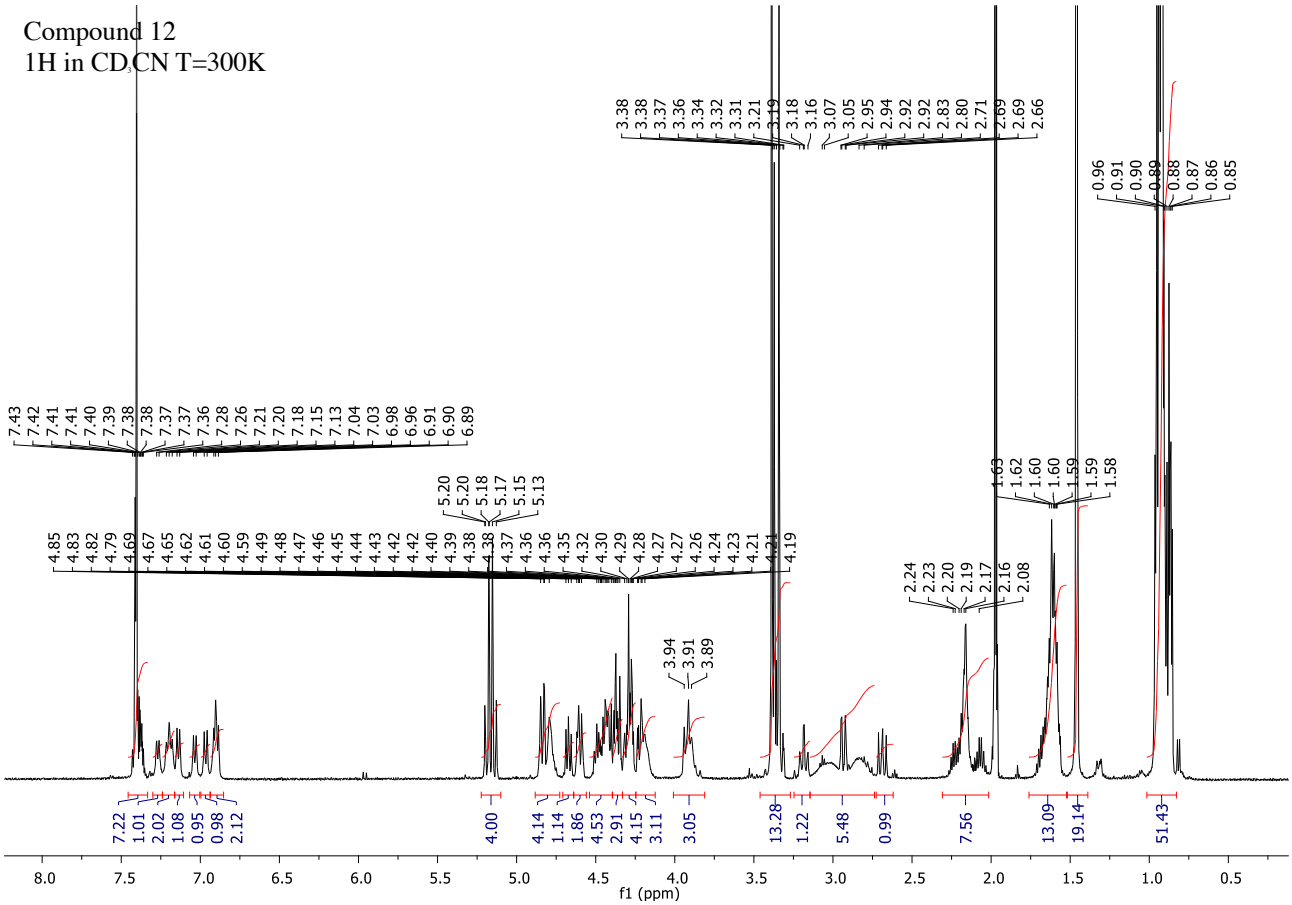

Compound 12
13C-APT in CD3CN a T=300K

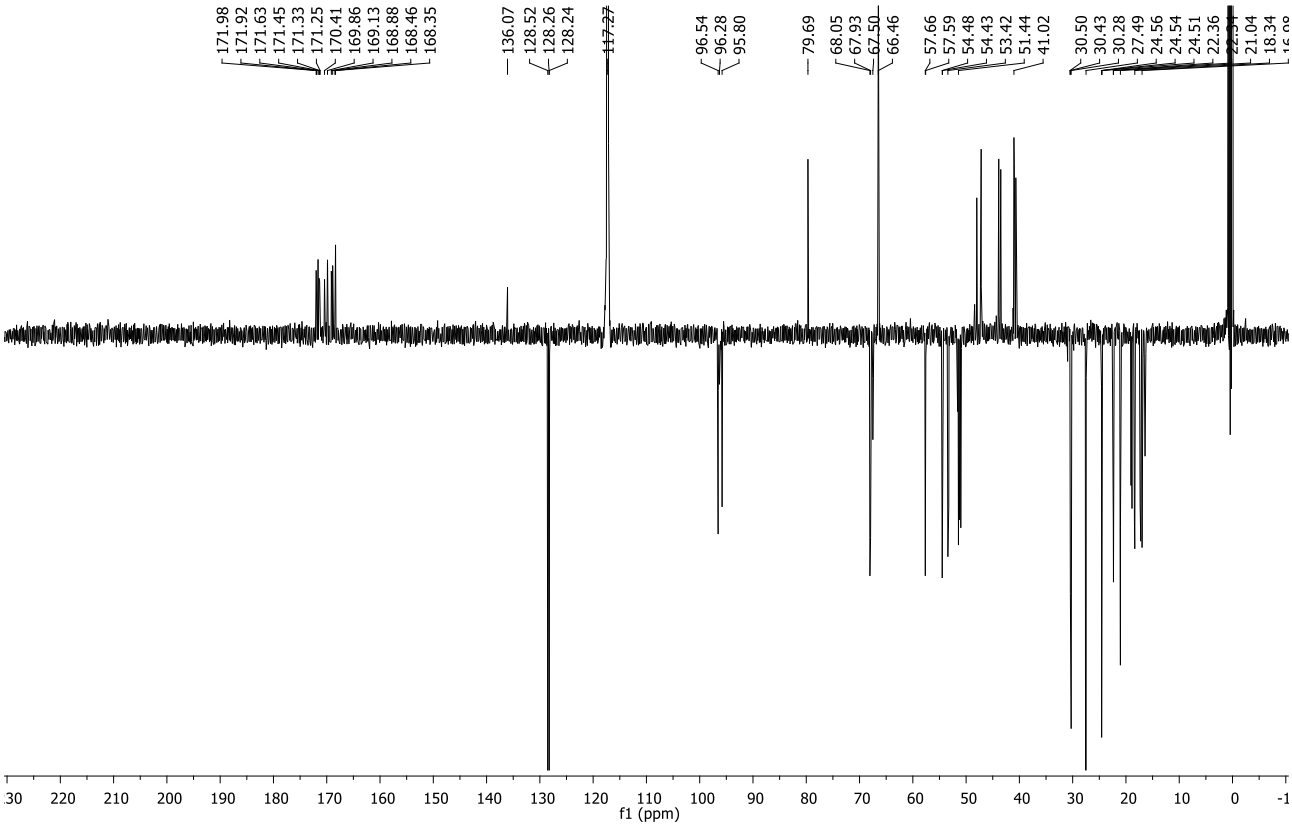

10. References

1 V. P. Romanova and V. V. Shilin, *Ukr. Khim. Zh.*, 1989, **55**, 527.
2 D. Steinke and M.-R. Kula, *Angew. Chemie*, 1990, **102**, 1204–1206.
3 P. A. Burland, H. M. I. Osborn and A. Turkson, *Bioorg. Med. Chem.*, 2011, **19**, 5679–5692.
4 F.-Y. Dupradeau, A. Pigache, T. Zaffran, C. Savineau, R. Lelong, N. Grivel, D. Lelong, W. Rosanski and P. Cieplak, *Phys. Chem. Chem. Phys.*, 2010, **12**, 7821–7839.
5 *Molecular Operating Environment (MOE), v2016.08*, Chemical Computing Group Inc., 1010 Sherbrooke St. West, Suite #910, Montreal, QC, Canada, H3A 2R7, 2016.
6 M. J. Frisch, G. W. Trucks, H. B. Schlegel, G. E. Scuseria, M. A. Robb, J. R. Cheeseman, G. Scalmani, V. Barone, B. Mennucci, G. A. Petersson, H. Nakatsuji, M. Caricato, X. Li, H. P. Hratchian, A. F. Izmaylov, J. Bloino, G. Zheng, J. L. Sonnenberg, M. Hada, M. Ehara, K. Toyota, R. Fukuda, J. Hasegawa, M. Ishida, T. Nakajima, Y. Honda, O. Kitao, H. Nakai, T. Vreven, J. Montgomery, J. A., J. E. Peralta, F. Ogliaro, M. Bearpark, J. J. Heyd, E. Brothers, K. N. Kudin, V. N. Staroverov, R. Kobayashi, J. Normand, K. Raghavachari, A. Rendell, J. C. Burant, S. S. Iyengar, J. Tomasi, M. Cossi, N. Rega, J. M. Millam, M. Klene, J. E. Knox, J. B. Cross, V. Bakken, C. Adamo, J. Jaramillo, R. Gomperts, R. E. Stratmann, O. Yazyev, A. J. Austin, R. Cammi, C. Pomelli, J. W. Ochterski, R. L. Martin, K. Morokuma, V. G. Zakrzewski, G. A. Voth, P. Salvador, J. J. Dannenberg, S. Dapprich, A. D. Daniels, Ö. Farkas, J. B. Foresman, J. V. Ortiz, J. Cioslowski and D. J. Fox, *Gaussian 09*, Gaussian Inc., Wallingford CT, 2009.
7 D. A. Case, D. S. Cerutti, T. E. Cheatham, III, T. A. Darden, R. E. Duke, T. J. Giese, H. Gohlke, A. W. Goetz, D. Greene, N. Homeyer, S. Izadi, A. Kovalenko, T. S. Lee, S. LeGrand, P. Li, C. Lin, J. Liu, T. Luchko, R. Luo, D. J. Mermelstein, K. M. Merz, G. Monard, H. Nguyen, I. Omelyan, A. Onufriev, F. Pan, R. Qi, D. R. Roe, A. Roitberg, C. Sagui, C. L. Simmerling, W. M. Botello-Smith, J. Swails, R. C. Walker, J. Wang, R. M. Wolf, X. Wu, L. Xiao, D. M. York and P. A. Kollman, *Amber 2017*, University of California, San Francisco, 2017.
8 J. A. Maier, C. Martinez, K. Kasavajhala, L. Wickstrom, K. E. Hauser and C. Simmerling, *J. Chem. Theory Comput.*, 2015, **11**, 3696–3713.
9 U. Doshi and D. Hamelberg, *J. Phys. Chem. B*, 2009, **113**, 16590–16595.
10 X. Grabuleda, C. Jaime and P. A. Kollman, *J. Comput. Chem.*, 2000, **21**, 901–908.
11 I. Maffucci, X. Hu, V. Fumagalli and A. Contini, *Front. Chem.*, 2018, **6**, 43.
12 T. Darden, D. York and L. Pedersen, *J. Chem. Phys.*, 1993, **98**, 10089–10092.
13 J.-P. Ryckaert, G. Ciccotti and H. J. C. Berendsen, *J. Comput. Phys.*, 1977, **23**, 327–341.